# Recent Advances in 1D Stretchable Electrodes and Devices for Textile and Wearable Electronics: Materials, Fabrications, and Applications

*Jaehong Lee, Byron Llerena Zambrano, Janghoon Woo, Kukro Yoon, and Taeyoon Lee\**

Research on wearable electronic devices that can be directly integrated into daily textiles or clothes has been explosively grown holding great potential for various practical wearable applications. These wearable electronic devices strongly demand 1D electronic devices that are light–weight, weavable, highly flexible, stretchable, and adaptable to comport to frequent deformations during usage in daily life. To this end, the development of 1D electrodes with high stretchability and electrical performance is fundamentally essential. Herein, the recent process of 1D stretchable electrodes for wearable and textile electronics is described, focusing on representative conductive materials, fabrication techniques for 1D stretchable electrodes with high performance, and designs and applications of various 1D stretchable electronic devices. To conclude, discussions are presented regarding limitations and perspectives of current materials and devices in terms of performance and scientific understanding that should be considered for further advances.

## 1. Introduction

Over the past decades, electronic devices have become smaller, which has improved their portability.[1,2] These trends in size and portability for electronic devices have naturally led to the rapid development of wearable electronics such as electronic skins, smart watches, and sport wristbands.[3–6] Among various types of wearable electronics, textile electronics which combine conventional textiles and electronic devices is one of attractive choices because clothes are essential at all times for all humans regardless of age or gender.[7–12] Therefore, many efforts have been made over the last decades to develop various textile electronics for wearable human–machine interfaces, biomedical

applications, and smart sportswear.[13–17] In this regard, stretchable and wearable electronic devices in the 1D form, which can be directly integrated into daily clothes without any inconsistency, are greatly promising for future wearable electronics.[18–23] In addition, the hierarchical property of the fibrous structures (fiber: a small and short piece of a strand, filament: a long strand, yarn: an intertwined 1D structure of fibers or filaments, and fabric: a flexible substance consisting of a network of yarns) makes 1D electronic devices and systems remarkably suitable for advanced wearable electronics. The 1D assemblies including the 1D electronic devices also have unique characteristics appropriate to wearable electronics such as softness, stretchability, breathability, and high tolerance to damage.[3]

Stretchability, in particular, is one of the most important properties for practical wearable applications because smart clothes or textiles including such 1D electronic devices should be covered on soft and curved human body.[24] Furthermore, some parts of clothes are frequently stretched and deformed during natural movements in daily life, thereby increasing the importance of stretchability of 1D electronic devices. Although many of existing clothes have achieved certain stretchability with only rigid yarns through specific textile structures such as woven or knitted structures, the stretchability resulting from such textile structures is insufficient to cover high stretchability desired in specific applications. For example, high stretchability of textiles is highly required for sportswear in order to achieve a form-fitting property, high comfortability, and elasticity during exercise. For such purpose, various stretchable yarns such as spandex have been widely used in textile industry. These properties of textiles are also essential for various sensing applications of wearable and textile electronic, resulting that high stretchability should be achieved for the 1D electronic devices.[25,26] In addition, the high stretchability resulting from the use of stretchable conductive yarns can successfully prevent a bagging issue of smart textiles which degrades stability and reproducibility of the smart textiles. For achieving the 1D stretchable electronic devices and systems, the development of 1D stretchable electrodes such as conductive yarns or filaments with high electrical conductivity and stretchability is basically essential above other things. In this regard, recent advances toward developing various high-performance

Dr. J. Lee, B. Llerena Zambrano
Laboratory of Biosensors and Bioelectronics
Institute for Biomedical Engineering
ETH Zurich
8092 Zurich, Switzerland
J. Woo, K. Yoon, Prof. T. Lee
School of Electrical and Electronic Engineering
Yonsei University
50 Yonsei-ro, Seodaemun-Gu, Seoul 03722, Republic of Korea
E-mail: taeyoon.lee@yonsei.ac.kr

1D stretchable conductive yarns are considerably remarkable based on the convergence of textile technologies, electronics, and nanotechnologies.[3,4] Although the achievements of 1D stretchable electronic devices are still not significant compared to those of the existing 2D stretchable electronic devices, the related fields have actively expanded because of the potential applications of this 1D stretchable electronics technology such as military garment devices, biomedical and antimicrobial textiles, smart sportswear, and personal electronics.[27–37]

This review article presents the status and state-of-the-art achievements in 1D stretchable electronics for advanced wearable electronics, which is expected to be one of main technologies in the areas of healthcare, environmental monitoring, human-machine interfaces, energy conversion and storage, and sports-biomechanics. The scope of this review article, which focuses on the 1D structure, comprehensively includes various fibrous structures such as fibers, filaments, and yarns. In addition, the term "stretchable" has been considered to a synonym of a term "elastic," including a capability to be restored to an original state as well as to be stretched. This review work is classified into roughly three sections reviewing the various conductive materials and fabrication approaches for 1D stretchable electrodes, and recent progress on representative 1D electronic devices based on the 1D stretchable electrodes. In the first section, carbon-based nanomaterials and metallic nanomaterials for 1D stretchable electrodes are introduced in terms of their characteristics, advantages, and limitations. Conventional and advanced fabrication techniques for the 1D stretchable electrodes are described in detail in the second section. In the third section, various 1D electronic devices based on 1D stretchable electrodes are presented—for example, mechanical sensors, environmental sensors, fiber heaters, and energy-harvesting and storage devices. The main goal of this review article is to provide a broad overview and understanding of 1D stretchable electrodes and their applications that have been developed in recent years. Although many review papers regarding 2D planar stretchable electronics and a few review papers about 1D fiber-based electronic devices have been published so far,[1,3–5,38–41] but to the best of our knowledge, there has been no review article mainly focusing on electronic devices which possess both 1D structure and stretchability. Finally, we summarize the review in the last part and present the perspectives and important issues that should be considered for commercial and practical applications beyond current conceptual prototypes. This review paper will be able to contribute to expand the research field by helping new researchers get into this field as a first review paper in this specific research field, accelerating advances of the research field by abundant human resources. In addition, based on the systematic summary of related research, limitations and perspectives of the field in this article, it is expected to be effectively leveraged by many researchers to advance the research field.

## 2. Conductive Materials for 1D Stretchable Electrodes

In general, the choice of materials used for fabricating 1D stretchable electrodes is based on electrically conductive components and elastic fibrous matrices. The selection of the

**Jaehong Lee** is currently working as a postdoctoral research fellow at the Laboratory of Biosensors & Bioelectronics (LBB) at ETH Zurich, Switzerland. He received his Ph.D. degree (2017) in electrical and electronic engineering from Yonsei University in the Republic of Korea. His Ph.D. thesis focused on developing various stretchable fiber electronics for wearable and textile electronics. His current research interests include 1D implantable soft electronics for biomedical and in vivo applications.

**Taeyoon Lee** is currently working as a professor in the School of Electrical and Electronic Engineering at Yonsei University, Republic of Korea. He received B.Sc. and M.S. degrees in metallurgical system engineering from Yonsei University in 1995 and 1997, respectively, and a Ph.D. degree in materials science and engineering from the University of Illinois at Urbana–Champaign, USA, in 2004. His research interests include bioengineering based on smart surfaces and fiber electronics for wearable and textile electronics.

conductive material plays the key role in realizing high electrical conductivity, stretchability, and mechanical stability of the electrodes. In such regard, a variety of conductive materials such as metal nanoparticles (NPs) and nanowires (NWs), carbon particles, carbon nanotubes (CNTs), and graphene have been proposed and investigated.[42–44] These materials can be categorized in two groups, namely, carbon-based nanomaterials and metallic nanomaterials. The current chapter will discuss the conductive materials used most frequently for fabricating 1D stretchable electrodes. These conductive materials are promising also for various other applications such as flexible, stretchable, and wearable electronics.

### 2.1. Carbon Nanomaterials for 1D Stretchable Electrodes

Various carbon-based nanomaterials with 1D and 2D structures have been widely used for flexible, stretchable and wearable electronics owing to their unique properties such as high electrical conductivities ($\approx 10^4$ S cm$^{-1}$), excellent intrinsic carrier mobility ($10^6$ cm$^2$ V$^{-1}$ S$^{-1}$), high flexibility and superior mechanical properties.[45] Based on their superior flexibility

**ADVANCED
SCIENCE NEWS**

www.advancedsciencenews.com

**ADVANCED
MATERIALS**

www.advmat.de

and high electrical performance, 1D stretchable electrodes have been mainly fabricated by use of graphene and CNTs among all carbon nanomaterials. Graphene is a one-atom-thick 2D layer of $sp^2$-bonded carbon allotrope with superb electrical and mechanical properties.[46] Although graphene can be synthesized by various methods, among them, graphene oxide (GO) is most widely used for 1D stretchable electrodes because GO can be readily synthesized and used through a simple solution-based process.[47] Li et al. used reduced GO (rGO) coated on an elastic fibrous matrix, as the conductive component for the 1D stretchable conductive electrode in stretchable electrothermal chromatic filament yarns.[48] The 1D electrodes presented an electrical resistivity of 0.02 Ωm and maintained stretching stability during 1000 repeated stretching/releasing cycles with the strains up to 60%, showing negligible degradation of conductivity after the repeated cycles. The electrical resistance of the yarn increased upon applying strain, leading to an increase in temperature due to the Joule effect. This phenomenon was then exploited to change the color of the yarns by using thermochromic inks that were stimulated by the heat produced by the flow of electrons in the rGO electrode. By prestretching the elastic matrix before coating, a higher amount of GO could be coated when the yarn was immersed in a GO solution. This was followed by the reduction of GO. This procedure resulted in lower resistivity and higher stretchability of the yarn caused by the increase in the amount of rGO in the yarn (**Figure 1**a,b). In a similar manner, Chang et al. fabricated graphene-based stretchable conductive yarns using a compressed spring architecture.[49] Polyester (PE) yarns were coated with GO and reduced to obtain rGO; subsequently, they were wound on a polyurethane (PU) yarn that served as an elastic filament scaffold. The sensor had an electrical conductivity of 0.136 S m$^{-1}$ and high stretchability of ≈100% (Figure 1c).

Although high electrical conductivity in 1D conductive electrodes is greatly desirable for achieving various high-performance 1D electronic devices, rGO is still limited by its relatively low electrical conductivity resulting from the abundance of structural defects in the lattice which come from the reduction process.[46] To address this issue, Wang et al performed thermal annealing treatment of rGO-based stretchable conductive yarns to remove the structural defects and improve the electrical conductivity.[50] The yarns were fabricated by twist-spinning thermally annealed rGO films. This process greatly improves the fracture strain up to 70% and increases the electrical conductivity remarkably to $6 \times 10^5$ S m$^{-1}$. These yarns were used as 1D stretchable heaters and they retained good electrical properties under tensile strains of up to 40% with low changes in resistance. The results of a Raman spectroscopy analysis showed that the $I_D/I_G$ decreases from 1.21 to 0.014 after annealing the fiber at 3000 °C. This proves that the structure is highly ordered structure and how the defects of rGO are greatly repaired (Figure 1d–f). The electrical properties of graphene can also be greatly improved by combining it with other materials. Gao and co-workers used a spring-like architecture made of a rGO/multi-walled CNTs (MWCNTs) composite.[51] The addition of MWCNTs with a considerably higher surface area increases the free electron availability and hence the current density in the 1D electrodes (Figure 1g). In addition to rGO, high-quality pristine graphene can also be produced by chemical vapor deposition

(CVD). This synthesis approach can avoid the harsh redox process of rGO synthesis, which induces numerous defects in the lattice. By using CVD, Hu and co-workers fabricated core-sheath CVD-grown graphene yarns by coating graphene on Cu wires.[52] After removing the Cu wires by etching, the graphene yarns were coated with polyvinyl alcohol (PVA), which imparted them flexibility and stretchability. The yarns exhibited conductive and mechanical properties higher than those reported for rGO-based conductive yarns. However, despite a high conductivity of $2.5 \times 10^4$ S m$^{-1}$, the stretching ability of the fabricated yarns only allowed a small strain of 7.1% before the fibers lost their electrical properties. The yarns underwent a constant relative change in resistance $\Delta R/R_o = 3$ when stretched to 6% for 200 cycles with no resistance degradation after strain release. This change is attributed to changes in the contact resistance of graphene sheets in the core, or at the interface of the polymer sheath and graphene core during deformation. Although graphene in its many forms can present excellent electrical properties, its high in-plane stiffness and high Young's modulus are obstacles for achieving high stretchability in conductive yarns for practical applications. However, graphene is not the only carbon allotrope with good mechanical and electrical properties, and researchers have also made explored alternatives (Figure 1h–i).

The stretchability of carbon nanomaterial-based 1D stretchable electrodes can be further improved by using higher aspect ratio materials. These materials can be used in 1D yarns to create a network where the numerous electrical contacts between the high-aspect-ratio materials provide a means to maintain electrical conductivity more effectively under stretching deformation. A representative example of such nanomaterials is carbon nanotubes. These are cylindrical nanostructures with high aspect ratio and remarkable electrical and mechanical properties. High electrical conductivities have been reported based on their nature and fabrication procedure, making them a good candidate for conductive materials of 1D stretchable electrodes.[53] Zhou et al. designed a thermoplastic elastomer (TPE) belt-like 1D stretchable electrode based on single-walled CNTs (SWCNTs).[54] The authors used wet-spun filament yarns with a solution of SWCNTs doped with acid in their core. After the acid was removed, the yarn was pressed on the surface to increase the density of electrical contacts in the core. Upon stretching, the yarns fragments with a high density of cracks were bridged by the SWCNTs, allowing the yarns to remain conductive over a long range. Although the initial electrical resistance of the yarns was ≈71 Ω cm$^{-1}$, which is not as low as that of other graphene-based yarns, they were able to withstand strains of up to remarkably high value of 250%. This behavior was explained by examining two regimes. For low strains (20%), the conductivity results from the dense contacts in the SWCNTs cracks. However, for higher strains, the network becomes increasingly disconnected, and electrons cannot flow through the cracks anymore; therefore, the only conduction path results from the SWCNTs covering the interface in the TPE sheath (Figure 1j). The appearance of cracks under strain can be easily observed particularly when the adhesive properties between the conductive material and the matrix are not optimal. In order to improve this aspect, Li et al. developed 1D stretchable conductive yarns by decorating carboxylic MWCNTs and SWCNTs on a thermoplastic polyurethane
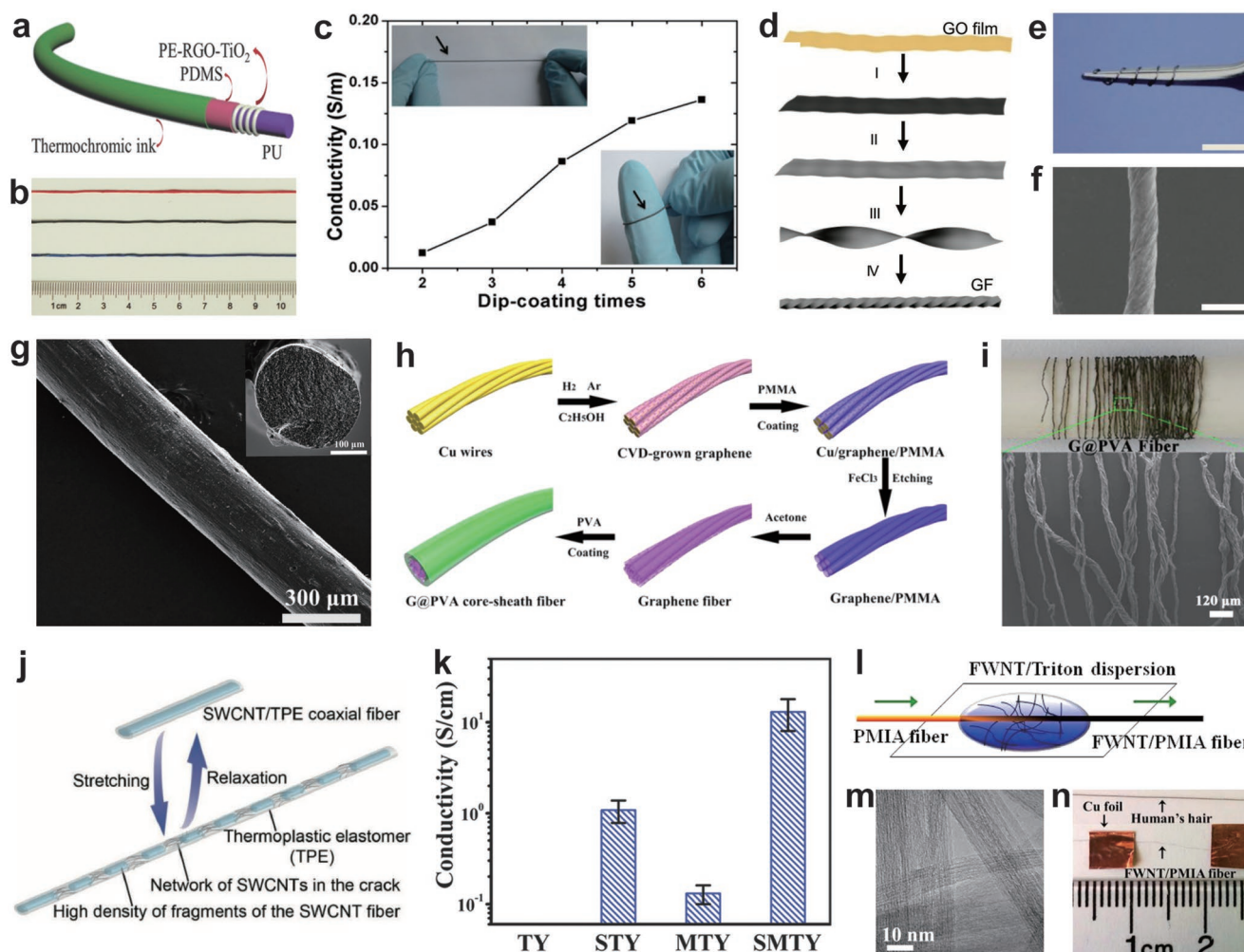
**Figure 1.** a) The schematic illustration of the structure of the stretchable electrothermal chromatic fiber using rGO, TiO$_2$, and PDMS. b) Photographs of the stretchable electrothermal chromatic fibers with different colors. (a,b) Reproduced with permission.[48] Copyright 2017, The Royal Society of Chemistry. c) Electrical conductivity of plasma-treated double coated yarn with rGO (PDCY-RGO) at varying dip-coating times. Reproduced with permission.[49] Copyright 2015, Wiley-VCH. d) Schematic illustration of the fabrication process of graphene-based conductive fibers. e) Optical image of the fabricated graphene-based conductive fiber. Scale bar is 1.5 cm. f) SEM image of a single graphene fiber with uniformly scrolled structure. Scale bar is 300 μm. (d–f) Reproduced with permission.[50] Copyright 2016, Wiley-VCH. g) Side-view SEM image of the rGO-based conductive fiber. Inset: cross-sectional SEM image of the rGO fiber. Reproduced with permission.[51] Copyright 2017, American Chemical Society. h) Schematic illustration of the fabrication process of graphene/PVA (G@PVA) fibers. i) Photograph and SEM image of a G@PVA fiber wound on a plastic rod. (h,i) Reproduced with permission.[52] Copyright 2015, American Chemical Society. j) Schematic presenting the fragmentation of the coaxial SWCNTs-based stretchable conductive fiber. Reproduced with permission.[54] Copyright 2018, Wiley-VCH. k) The conductivity comparison of various stretchable conductive fibers based on SWCNTs, MWCNTs, and their mixture. Reproduced with permission.[55] Copyright 2018, The Royal Society of Chemistry. l–n) Schematic illustration of the preparation of the FWCNTs/PMIA stretchable conductive fiber, TEM image of FWCNTs, and optical image of FWCNTs/PMIA fiber compared with a human hair, respectively. Reproduced with permission.[57] Copyright 2015, American Chemical Society.

composite (TPU).[55] The stretchable TPU filament yarn was first decorated with MWCNTs to achieve an electrical conductivity of 0.13 S cm$^{-1}$, which is almost ten times less than that of yarns with only SWCNTs (1.08 S cm$^{-1}$). Subsequently, the TPU yarn was first coated with MWCNTs and then with SWCNTs (3.65 wt%) to increase the conductivity (13 S cm$^{-1}$) by 100 times compared to the yarns coated with MWCNT and by 12 times compared to the ones coated with SWCNTs. The adsorption of carboxylic MWCNTs on the TPU yarns enhanced the hydrophilic performance of the yarns and promoted SWCNTs attachment, which in turn increased the conductivity

and allowed maintaining stable conductivity under strains of up to 100% (Figure 1k). To further increase the conductivity, few wall CNTs (FWCNTs), i.e., CNTs with two to five layers of carbon atoms, have also been used because of their high electrical and mechanical properties and cost-efficient synthesis.[56] Jiang et al. used randomly distributed FWCNTs coated in a poly (m-phenylene isophthalamide) (PMIA) matrix for 1D stretchable conductive yarns.[57] The electrical conductivity of the yarn was effectively increased from 10.97 to 101.50 S cm$^{-1}$ by applying different annealing temperatures for the yarns. The enhancement of the conductivity by annealing could be

**ADVANCED
SCIENCE NEWS**

www.advancedsciencenews.com

**ADVANCED
MATERIALS**

www.advmat.de

attributed to the improved adhesion and interaction between the matrix and the FWCNTs and possible evaporation of the surfactant from the FWCNTs, thereby decreasing the contact resistance. The FWCNTs in the annealed yarns tend to align in the strain direction during deformation, increasing the electrical stretchability of the yarns. (Figure 1l–n).

Even though the high electrical and mechanical properties of carbon-based nanomaterials, such as CNTs and graphene, are quite appealing for fabricating 1D stretchable electrodes, their practical use for achieving high electrical performance still faces many challenges. As an alternative, metallic nanomaterials offer many attractive features and options that can employed to enhance the electrical performance of 1D stretchable electrodes. In the following subsection, we will discuss in more detail the use of various metallic materials as electrical conductors in 1D stretchable conductive yarns.

## 2.2. Metallic Nanomaterials for 1D Stretchable Electrodes

Although metals have generally limited mechanical flexibility compared to carbon-based nanomaterials, metallic nanomaterials such as NPs and NWs, can act as excellent conductive materials for 1D stretchable electrodes, providing the yarns with high mechanical flexibility and electrical conductivity. Because a typical approach for using conductive nanomaterials for 1D stretchable electrodes is based on the percolation or network of the nanomaterials, 1D metallic NWs have been widely investigated for fabricating 1D stretchable electrodes due to their high aspect ratio. The high aspect ratio of NWs ensures the network of NWs to maintain the electrical contacts between the NWs under high tensile strain, imparting high electrical stretchability to the conductive yarns. Chen et al. used AgNWs to create a 1D stretchable conductive yarn for strain-sensing by combining AgNWs with a poly(vinylidenefluoride-co-trifluoroethylene) (P(VDF-TrFE)) polymer nanofiber mat, which was previously coated on a prestretched elastic filament yarn.[58] By increasing the contents of AgNWs in the yarn, a high electrical conductivity of 5 $\Omega$ cm$^{-1}$, stretchability greater that 100% high stability over 10 000 strain cycles of 90% with negligible change in its sensitivity were realized (**Figure 2**a). Lu et al. also used AgNWs to fabricate 1D stretchable conductive yarns.[59] They obtained higher electrical conductivities and stretching ranges by modifying the surface of AgNWs to greatly improve the compatibility with a stretchable PU matrix. Particularly, they improved the dispersion of AgNWs in the liquid PU matrix in order to create a more homogeneous network for a wet-spun composite. They compared the electrical conductivity of yarns with and without modified AgNWs and found that the conductivity of yarns without surface modification was 147 S cm$^{-1}$, while that of yarns with modified NWs was 331 S cm$^{-1}$. The highest conductivity obtained by increasing the percentage by weight concentration of modified AgNWs was 7330 S cm$^{-1}$. In addition, the yarns were able to remain conductive under strains up to ≈140%. The outstanding conductivities realized by Lu et al. are the consequence of a uniformly dispersed AgNWs network, resulting from the improved dispersibility of the AgNWs after coating with a polyethylene Glycol (PEG) derivative (Figure 2b–d). Sun and co-workers also used a AgNWs/PU

composite yarn with sheath-core architecture.[60] In this work the authors were able to obtain yarns with initial resistance lower than 1 $\Omega$ cm$^{-1}$. The resistance of these yarns changes only by 10% upon applying a strain of 110%. Thus, these yarns were suitable for use as stretchable conducting wires. The key aspect of this work is the control of the stretching properties by focusing on the width of the interface of the coating between the conductive NWs and the elastic matrix which highlights the importance of not only the conductive material, but the system as a whole (Figure 2e–g).

In addition to 1D nanomaterials, NPs can also be additionally incorporated into 1D stretchable electrodes. Lee et al. used both AgNPs and AgNWs as conductive fillers in an styrene–butadiene–styrene (SBS) elastomeric matrix.[61] As a result, they obtained composites with an initial conductivity of 2450 S m$^{-1}$; these composite could withstand strains of up to 220% without losing conductivity. This electrical stretchability is higher than the theoretical value based on the 3D percolation theory. The high stretchability is attributed to the AgNWs-bridges between the networks of AgNPs disconnected by the applied strain. The synergetic effect of AgNPs and AgNWs depended on the length of the AgNWs, with higher stretching ranges and conductivities being observed for longer AgNWs. This finding highlights the importance of AgNWs in realizing long stretching ranges (Figure 2h,i). Although high stretchability is generally related to the use of high-aspect-ratio materials, Lee and co-workers achieved outstanding performance for 1D stretchable conductive yarns by only using NPs.[24] They incorporated AgNPs into a PU stretchable filament yarn by reducing large amounts of Ag ions previously absorbed in the yarn into AgNPs. The fabricated yarns presented a remarkably high conductivity of 20 964 S cm$^{-1}$; this conductivity was achieved on the number of times the yarns underwent reduction. The reduction process enabled generating a large number of AgNPs inside and outside the yarn, imparting the yarn with a remarkable strain range of up to 450% and stability over 10 000 stretching cycles. These properties were realized without using any high-aspect-ratio nanofillers such as NWs (Figure 2j). Baik and co-workers also reported the creation of 1D stretchable conductive yarns using Ag nanoflowers as a conductive filler in a wet-spun PU filament yarn.[62] In this case too, the use of a single-type filler was enough to achieve excellent electrical conductivity and mechanical properties. The obtained conductivity was 41 245 S cm$^{-1}$, which is one of the highest reported as yet, and the rupture strain was 90%. The excellent performance of the yarns was attributed to the higher surface area of the nanoflowers compared to the area of NWs and NPs. (Figure 2k)

Ag is the most commonly used metal for fabricating 1D stretchable electrodes owing to its outstanding electrical properties; however, other metals such as Au and Cu have also been investigated for forming 1D stretchable electrodes. Cheng et al., used CuNWs to create 1D stretchable conductive yarns with high conductivity.[63] The CuNWs were coated onto a helical yarn made by PE microfibers. The electrical conductivity of the yarns was improved by using H$_2$ plasma, which removed the organic residues and oxide layers. In addition, nanowelding between the CuNWs in the network decreased the contact resistance and granted the yarn a low electrical resistance of 2.5 $\Omega$ cm$^{-1}$ to the yarns (Figure 2l). Moreover, taking

**ADVANCED
SCIENCE NEWS**

www.advancedsciencenews.com
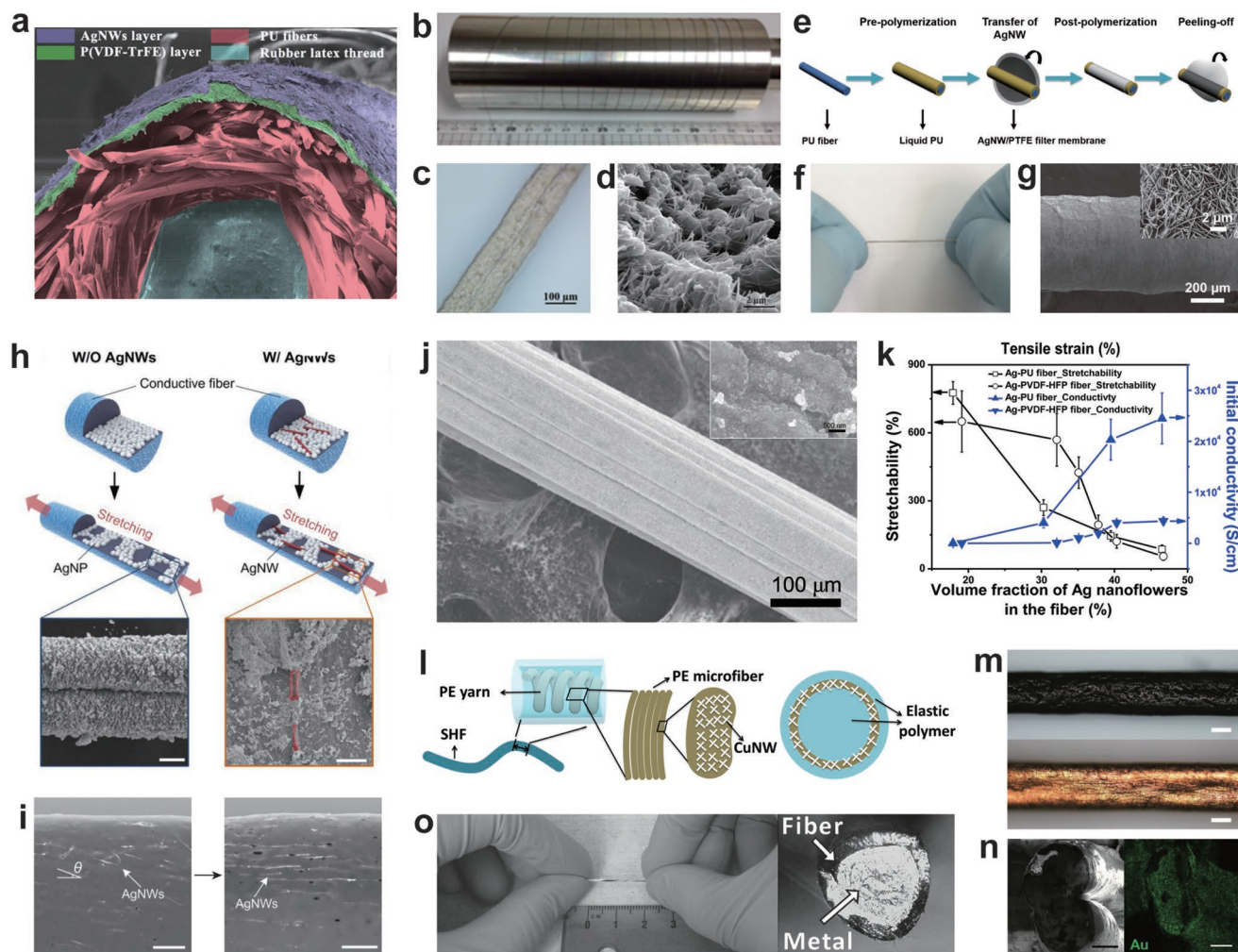
**ADVANCED
MATERIALS**

www.advmat.de

**Figure 2.** a) Cross-sectional SEM image of the stretchable conductive fibers using AgNWs, P(VDF-TrFE) nanofiber mats, and elastic fiber substrate. Reproduced with permission.[58] Copyright 2016, Wiley-VCH. b) Photograph of the stretchable conductive fibers based on the surface-modified AgNWs and PU composite. c) The optical microscope image of the fiber in reflection modes. d) Cross-sectional SEM image of the composite fiber. (b–d) Reproduced with permission.[59] Copyright 2018, American Chemical Society. e) Schematic illustration of the fabrication process for the AgNWs/PU stretchable conductive fiber. f,g) Photograph and SEM images of the fabricated AgNWs/PU stretchable conductive fiber, respectively. (e–g) Reproduced with permission.[60] Copyright 2018, American Chemical Society. h) Schematic illustration of changes in AgNWs and AgNPs in the stretchable conductive fibers under stretching. (Left navy-lined box: SEM image of the AgNPs-mixed SBS fiber without AgNWs at 50% strain. Scale bar = 30 μm. Right red-lined box: SEM image of the 0.56 wt% AgNWs–AgNPs embedded SBS fiber at 50% strain. Scale bar = 4 μm). i) Backscattered SEM images of the 0.56 wt% AgNWs-mixed SBS fibers without AgNPs at pre- and 50% strains (Scale bars = 20 μm). (h,i) Reproduced with permission.[61] Copyright 2015, Wiley-VCH. j) SEM images showing the surface of the stretchable conductive fibers based on AgNPs. The inset: the higher-magnification SEM image showing the uniform formation of AgNPs. Reproduced with permission.[24] Copyright 2018, American Chemical Society. k) Effect of Ag nanoflower concentration on stretchability and conductivity of stretchable conductive fibers. Reproduced with permission.[62] Copyright 2015, American Chemical Society. l) Schematic illustration of the hierarchical structure of the stretchable conductive fibers based on CuNWs. Reproduced with permission.[63] Copyright 2016, American Chemical Society. m) The optical microscope image of the AuNWs/SEBS fiber before and after the growth of gold film on the fiber, respectively (scale bars = 100 μm). n) Cross-sectional SEM image and the corresponding EDX mapping image of the AuNWs/SEBS fiber after the growth of the gold film. (m,n) Reproduced with permission.[64] Copyright 2018, Wiley-VCH. o) Photograph of the ultrastretchable conductive fiber based on LM. The inset: The shiny core of its cross-section is the LM. Reproduced with permission.[66] Copyright 2012, Wiley-VCH.

inspiration from moss, Zhao et al. used AuNWs as seeds in an elastic yarns to grow Au films by electroless deposition.[64] The yarns showed electrical conductivities of up to 461 S cm$^{-1}$. Their conductivities could increase or decrease on application of strain, depending on the amount of prestrain used during the fabrication process (Figure 2m,n).

An interesting available alternative is the use of liquid metal (LM) alloys with very low melting points that are a liquid at room temperature.[65] These materials flow in response to deformation and effectively maintain their electrical conductivity under tensile strain. Zhu et al. fabricated a 1D stretchable electrode by injecting EGaIn into poly[styrene-(ethylene-co-butylene)-styrene] (SEBS) hollow filament yarns.[66] The introduction of LM has negligible impact on the mechanical properties of the yarn. The fabricated yarn presented a very low electrical resistivity of $3 \times 10^{-5}$ Ω cm$^{-1}$ and electrical

stretchability under a strain of up to 800%. The change in electrical resistance upon application of tensile strain is caused by the increase in yarn length as the cross-sectional area decreases. Such behavior is one of the advantages of using LMs for stretchable conductive yarns as LMs can be treated as normal wires, thereby facilitating the development of theoretical models (Figure 2o).

Thus, a wide variety of metals and alloys can be used for fabricating 1D stretchable electrodes, and the obtained 1D stretchable electrodes have better performance compared to the performance of carbon-based nanomaterials. The wide variety of options not only include many types of metallic materials such as silver, gold, and copper, but also cover materials of different shapes and dimensions (NPs, NWs, nanoflowers, and LM). In terms of the performance, the materials presented in this subsection show higher conductivities and stretchabilities compared to CNTs- or graphene-based fibers. Many factors can be responsible for the high performance of metallic nanomaterial-based stretchable conductive fibers. For example, the contact resistance between the conductive nanomaterials in the yarn can be one of the reasons. Although carbon-based materials too may realize high conductivities, the contact resistance between CNTs or different graphene sheets is generally higher than that observed in metals.[67]

## 3. Fabrication Techniques for 1D Stretchable Electrodes

The fabrication method for 1D stretchable electrodes is one of the important considerations because various parameters such as performance, stability, cost, and efficiency of the electrodes are determined by its fabrication method. Typical fabrication methods for 1D stretchable conductive yarns are based on forming conductive composites composed of conductive materials and elastomeric materials in the form of yarns, or coating conductive materials on the surface of polymeric yarns. The following section will present three types of representative fabrication strategies for 1D stretchable electrodes.

### 3.1. Direct Spinning Methods of Stretchable Yarns with Conducting Materials

In order to fabricate stretchable conductive composites in the form of yarn, the direct extraction of the mixture of conductive materials and elastomeric matrix into yarn form has been widely investigated by using various conventional spinning methods such as wet spinning, dry spinning, and thermal drawing method. The wet-spinning method is a scalable production technology for filament yarns, and it is widely employed in industry. Filament yarns are fabricated by injecting a base polymeric solution through a nozzle into a coagulation bath at an appropriate rate. Stretchable conductive yarns can also be effectively fabricated by adding conductive materials into a polymeric solution and extracting the mixture into a filament form by the wet spinning method.[68–70] Ma et al. fabricated stretchable conductive yarns with high electrical properties by the scalable wet spinning method (**Figure 3**a).[62] A mixture of flower-shaped AgNPs with nanodisc-shaped petals

(Ag nanoflowers) and PU elastomer was extracted into a yarn composite by the wet spinning method to obtain stretchable conductive yarns. An outstanding electrical conductivity was achieved by the Ag nanoflowers, which is two orders of magnitude higher than that of fibers based on typical spherical AgNPs. However, there existed a trade-off relationship between the electrical conductivity and stretchability of the stretchable conductive yarns according to the conductive filler fraction. Based on the wet spinning method, stretchable conductive yarns with a core-sheath structure were developed by using a coaxial nozzle.[54,71] Tang et al. developed a facile and scalable one-step coaxial wet spinning assembly strategy to fabricate core-sheath stretchable conductive yarns; even MWCNT core protected by the silicone elastomeric sheath could be used (Figure 3b).[71] The fabricated conductive yarns were insulated by the elastomeric sheath similar to conventional cables and also possessed high stretchability over 300%, excellent stability, negligible hysteresis, fast response time, and washability. Zhou et al. also designed a coaxial wet spinning and post-treatment approach to fabricate stretchable conductive coaxial yarns including filaments with thermoplastic elastomer-wrapped SWCNTs core (Figure 3c,d).[54] The SWCNTs core was densified by applying pressure on the surface of the fibers after fabrication, resulting in a belt-like coaxial yarn with high performance.

A dry spinning method, typically used for the large-scale industrial production of filament yarns, has also been investigated to develop stretchable conductive yarns.[64,72–74] In the dry spinning method, polymeric filaments are extracted by extruding the source polymer solutions in a volatile solvent into a warm air environment through the nozzles. Although this process often involves hazardous flammable solvents, it is robust to impurities during the process. Further, this process is faster than the wet spinning method. Zhao et al. developed stretchable conductive yarns with high conductivity and stretchability by using a dry spinning method and an ultrathin AuNWs-seeded electroless deposition strategy (Figure 3e,f).[64] The AuNWs were well mixed with an highly elastic SEBS block copolymer to form AuNWs/SEBS stretchable yarns through the dry spinning method. The AuNWs in the yarn could act as seeds to achieve conformal electroless deposition of Au films on the surface of the yarns, forming a strong adhesion between the Au films and elastomeric yarns. To achieve high stretchability, the yarns were prestrained before the electroless deposition of the Au films, forming directional cracks and wrinkles along the axis of the deposited Au films. Based on the smoothening of wrinkles and self-repairing of cracks according to the applied strain, the electrical conductivity of the yarn was drastically improved to exceed 600% when the yarn was stretched under 380% strain (Figure 3g). By using a modified dry spinning method, Ma and co-workers developed ultra-stretchable, anti-freezing, conductive hydrogel yarns by mimicking the hierarchically organized structure of spider silk fiber (Figure 3h–i).[72] Both crystalline and amorphous domains of polymer chains are included in the yarns, providing a large stretchability of ≈1200%, fast resilience of under 30 s, and high tensile strength of 5.6 MPa. In addition, the fabricated stretchable yarn showed an electrical conductivity of 2 S m$^{-1}$ because of the polyelectrolyte nature of sodium polyacrylate (PAAS) in the hydrogel yarns (Figure 3j).
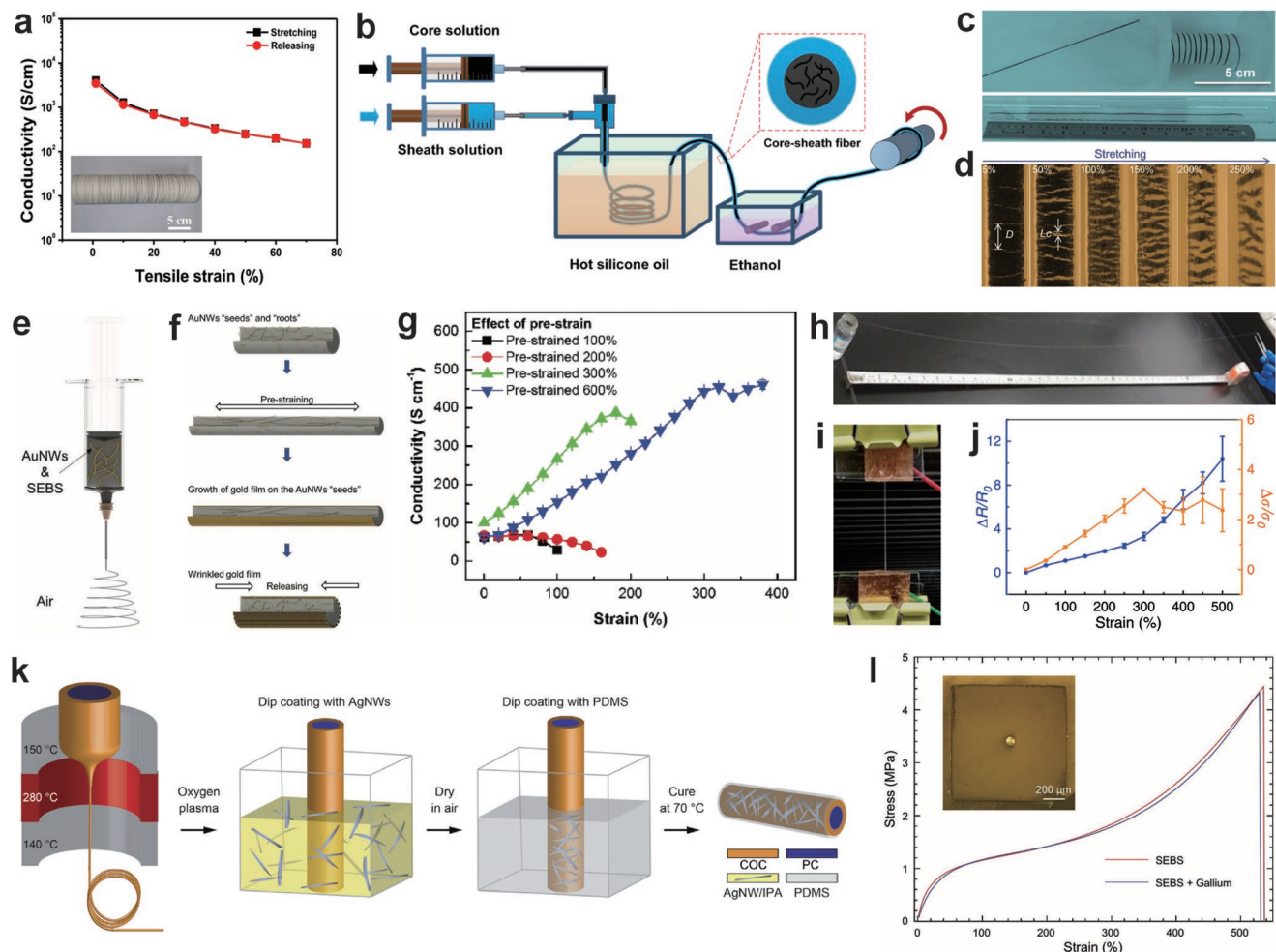
**Figure 3.** a) Conductivity–strain relationship of the stretchable conductive fiber fabricated from the wet-spinning method. The inset: Fiber collected on a winding drum (length ≈50 m). Reproduced with permission.[62] Copyright 2015, American Chemical Society. b) Schematic illustration of the coaxial wet-spinning process for the stretchable conductive fibers. Reproduced with permission.[71] Copyright 2018, American Chemical Society. c) Photographs of the fabricated coaxial stretchable conductive fiber. d) Photograph of the coaxial stretchable conductive fiber when stretched from 5% to 250% strain. $D$ and $L_c$ represent the average spacing between the cracks and average crack opening displacement, respectively. (c,d) Reproduced with permission.[54] Copyright 2018, Wiley-VCH. e) Schematic illustration of the dry-spinning process to fabricate AuNWs/SEBS stretchable conductive fibers. f) Schematic illustration of the formation of AuNWs-rooted continuous gold films on the fiber surface. g) The conductivity–strain curves on the effect of prestrain levels of the stretchable conductive fibers. (e–g) Reproduced with permission.[64] Copyright 2018, Wiley-VCH. h) Photograph of a 1.1 m-long as-prepared stretchable conductive fiber fabricated by the dry-spinning method. i) Photograph of the fabricated fiber showing its high stretchability. j) Relative resistance variation and relative conductivity variation of the stretchable conductive fibers under stretching. (h–j) Reproduced under the terms of the Creative Commons CC BY 4.0 license.[72] Copyright 2018, The Author(s), published by Springer Nature. k) Schematic illustration of the thermal drawing method for stretchable conductive fibers. Reproduced with permission.[81] Copyright 2017, The Authors, some rights reserved; exclusive licensee American Association for the Advancement of Science. Distributed under a Creative Commons Attribution NonCommercial License 4.0 (CC BY-NC). l) Stress–strain curves of a pure SEBS fiber and an SEBS fiber filled with LMs, of which the optical microscope image is shown in the inset. Reproduced with permission.[82] Copyright 2018, Wiley-VCH.

The thermal drawing method, which was initially developed and used for optical fibers, has been recently investigated for fabricating stretchable conductive filament yarns.[75,76] In the thermal drawing method, functional filaments can be effectively extracted with high throughput by passing the preform of filament with a large diameter into a furnace. Fink group advanced the thermal drawing method as a powerful tool for various multifunctional filaments for optical, electrical, chemical and bioelectronic applications.[77–81] For electrophysiological recoding, Lu et al. developed flexible and stretchable optoelectronic probing fibers from the mouse spinal cord by using the thermal drawing method (Figure 3k).[81] The cyclic olefin copolymer elastomer with a low modulus of 34 MPa and a melting point of 84 °C was used to overcome the limitations of the existing rigid probes fabricated by a thermal drawing process. The stretchable filaments exhibited a low impedance of 34 ± 17 kΩ, within the suitable range for extracellular recording application. This impedance was realized by coating AgNWs mesh electrodes on the surface of the filaments. In addition, the fabricated stretchable filament yarns maintained low impedance

at strains up to 100%, thus exhibiting better performance than that observed in their practical application. In the case of the thermal drawing method, the structures and components of the fabricated yarn can be readily controlled by adjusting the preform of the fiber, thereby allowing the successful application of this process for various multi-material and structure yarns. Qu et al. designed superelastic conductive yarns that were hundreds of meters long via the thermal drawing method.[82] Even though elastomeric materials have been limited in the thermal drawing process for multi-material yarn, they developed a multi-material thermal drawing process using thermoplastic elastomers based on an appropriate rheological and microstructure analysis. The stretchable conductive yarns were fabricated by co-drawing SEBS with an electrically conducting thermoplastic composite, namely, carbon black-loaded polyethylene, or by filling liquid metal into the hollow channels of stretchable yarns fabricated by the thermal drawing process. The fabricated stretchable conductive yarns could not only sustain up to a high strain of 500%, but also effectively maintain their electrical properties under high tensile strains (Figure 3l). This methodology potentially can help fabricate various multi-material and multifunctional elastic yarns at large scalability and low cost, suggesting the process as one of the leading technologies for the fabrication of stretchable conductive yarns in various applications.

### 3.2. Coating, Physical, and Chemical Incorporation of Conducting Materials

Stretchable conductive composites can be directly fabricated in the form of yarn by using various conductive materials in several spinning methods as described in the previous section. However, the limited uniformity of the percolated conductive materials and demand for using the industrially verified yarns still remain as challenges in some cases. In this regard, various approaches to endow conductivity to the previously fabricated elastic yarns such as a dip coating, physical deposition, and chemical reduction method have been investigated.

The dip-coating process is a widely used solution-based coating process. This process is simple, fast, and cost-efficient.[83–85] In the dip-coating process, it is important to not only prepare a solution in which the materials to be coated are uniformly dispersed, but also ensure that the coated material is firmly fixed without delamination from the substrate. Wang et al. designed a scalable fabrication process to fabricate stretchable conductive yarns by repeatedly dip-coating SWCNTs on the surface of the elastic PU/cotton core-spun yarn (**Figure 4**a,b).[86] The elastic core-spun yarn was fabricated by entwining cotton sheath yarns around highly elastic PU filament; subsequently, the yarn was passed through the well-dispersed SWCNTs solution. For ensuring high uniformity during dip-coating and adhesion between the coated SWCNTs and the elastic filament, two strong hot wind dryers were immediately used to quickly evaporate the solvent of the CNT ink. The electrical conductivity of the fabricated yarn was increased by repeating the dipping process of the SWCNTs on the elastic filaments. In addition, the stretchable conductive yarns exhibited high stretchability up to a tensile strain of 300% and reliable long-term cycling stability for nearly 300 000 cycles. Li et al. also

developed stretchable conductive yarns by coating a conductive AgNP/graphene-microsheet composite sheath, and a elastomeric encapsulation layer on an elastic PU core filament (Figure 4c).[87] The graphene-microsheets were repeatedly dip-coated on the surface of the pretreated elastic PU filament, providing the electrical conductivity of 60.5 mS cm$^{-1}$. The electrical conductivity of the fabricated yarn could be further improved to 423.7 mS cm$^{-1}$ by additionally depositing AgNPs. Using a modified dip coating process, Busfield and co-workers proposed a straightforward method to fabricate conductive cords by incorporating CNTs into the elastomeric adhesive layer dip-coated on the surface of glass fibers.[88] Based on its electrical conductivity of 10$^{-2}$ S m$^{-1}$, the percolated CNTs network provided a self-sensing ability for interfacial strain and damage in the cord-rubber composites under the external stress. The dip-coating method is promising from the viewpoint of simple, fast, low cost, and scalable fabrication. However, some challenges still persist with regard to the limited electrical performance and poor stability against external mechanical stimulations.

Zhang et al. proposed a novel and convenient rolling strategy to prepare high-performance stretchable conductive yarns based on the physical deposition of Au films (Figure 4d,e).[89] The stretchable conductive yarns were fabricated by rolling a Au/polydimethylsiloxane (PDMS) thin film in a spiral structure. By using the simple rolling strategy and restricting the crack elongation by an encapsulation effect of the spiral structure, a cracking control strategy is achieved; the size of the Au film cracks was reduced and more conductive pathways were effectively maintained during the stretching of the yarn. Therefore, the Au films deposited in the yarn underwent only small changes in resistance in the stretching stimulation. In particular, the resistance change of the fiber was about 1.5 under 50% strain, which is less than that of a thin film at the same strain (Figure 4f). Although this novel approach provides high electrical conductivity for metal films and excellent electrical stretchability using the cracking controlling strategy, continuous and scalable fabrication is still desired in this method.

Recently, a chemical reduction approach which can incorporate inorganic conductive materials into elastomeric polymers, was applied for forming high-performance conductive yarns.[24,61,90] By this approach, a large number of inorganic NPs can be uniformly distributed inside elastomeric yarns by absorbing metal precursors and then reducing them by using reducing agents. This approach has unique advantages in terms of the high efficiency of the process, high performance of the product, and fast and simple fabrication. Lee and co-workers, for the first time, applied a chemical reduction process to fabricate high-performance conductive yarns with low electrical resistance and high stability against external mechanical stimulations at the same time (Figure 4g).[90] The conductive yarns were fabricated by absorbing many Ag ions into the elastomeric polymer (SBS) coated on commercial Kevlar fibers and reducing the absorbed Ag ions into AgNPs inside the SBS layer. The fabricated conductive fibers exhibited a low electrical resistance of 0.15 Ω cm$^{-1}$ based on the large number of AgNPs incorporated in the SBS layer (Figure 4h) and high stability over more than 10 000 bending cycles. In a similar manner, the chemical reduction process was also
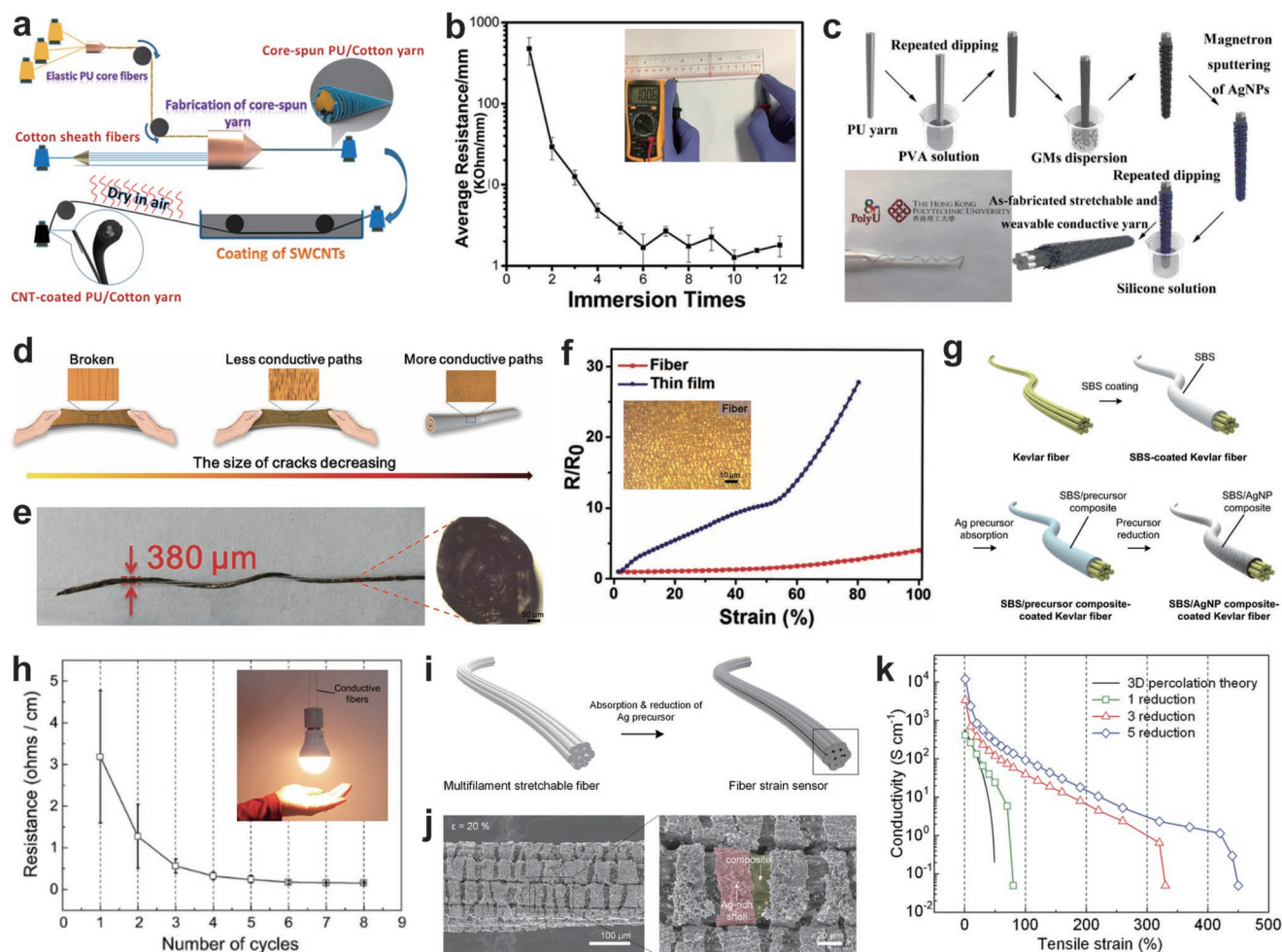
**Figure 4.** a) Schematic illustration of the self-developed fabrication process based on the dip-coating process for the PU/cotton/CNT-based stretchable conductive fibers. b) Electrical resistance of the stretchable conductive fiber versus the number of dip-coating. (a,b) Reproduced with permission.[86] Copyright 2016, American Chemical Society. c) Schematic illustration of fabrication process for the stretchable conductive fibers based on the dip-coating of conductive materials. Reproduced with permission.[87] Copyright 2018, Springer Nature. d) Schematic illustration showing the principle of reducing the length and width of the cracks in the Au-based stretchable conductive fiber, which provides low resistance change while stretching. e) Photograph of the fabricated stretchable conductive fiber. Right image shows the cross-sectional optical microscope image of the fiber. f) The stretchability and resistance change of the fabricated fiber and thin film. The inset: Morphology of cracks in the fiber. (d–f) Reproduced with permission.[89] Copyright 2018, Wiley-VCH. g) Schematic illustration of the fabrication of the conductive fiber through chemical reduction process. h) Electrical resistance changes of the conductive fiber according to the cycles of absorption and reduction of Ag ions. The inset: photograph showing emission of a light bulb connected to the conductive fiber. (g,h) Reproduced with permission.[90] Copyright 2015, Wiley-VCH. i) Schematic illustration of the fabrication process for the AgNPs-based stretchable conductive fiber through the chemical reduction process. j) SEM images of the surface of the stretchable conductive fibers under stretching. The fiber exhibits a Ag-rich shell region that grabs the inner composite (highlighted in red) and an inner composite region that is exposed (highlighted in yellow). k) Electrical conductivities of the stretchable conductive fibers under various conditions and calculated conductivity of the fiber using the classical 3D percolation theory according to the applied strain. (i–k) Reproduced with permission.[24] Copyright 2018, American Chemical Society.

used to fabricate the stretchable conductive yarns by incorporating AgNPs inside the elastomeric SBS filament extracted by the wet spinning method with AgNWs.[61] More conductive materials can be additionally embedded into conductive composites, and hence, the performance of the stretchable conductive yarn can be further improved by the chemical reduction process.

In the case of the conductive composites composed of conductive fillers and elastomeric matrix, the degradation of electrical conductivity under tensile strains can be theoretically explained by the 3D percolation theory and the classical power-law relationship.[91,92] In particular, the electrical conductivity of conductive composites can be calculated by

$$\sigma = \sigma_0 \left( V_f^0 - V_c^0 \right)^s \tag{1}$$

where $\sigma$ is the electrical conductivity of the conductive composites, $\sigma_0$ is the bulk conductivity of the conductive filler, $s$ indicate the critical exponent, $V_f^0$ and $V_c^0$ mean the volume

**ADVANCED
SCIENCE NEWS**
www.advancedsciencenews.com

**ADVANCED
MATERIALS**
www.advmat.de

fraction of the filler and percolation threshold without external strain, respectively. The percolation threshold of conductive composites ($V_c^0$) can also be calculated using the average interparticle distance model as follows[93]

$$V_c^0 = \frac{\pi D^3}{6(D+D_{IP})^3} \qquad (2)$$

where $D$ is the diameter of the conductive fillers and $D_{IP}$ is the distance of electric tunneling. In addition, the volume fraction of conductive fillers in the composites is readily determined by the ratio between the volume of conductive fillers in the composites and the total volume of the composites as follows

$$V_f = \frac{V_{conductive\ fillers}}{V_{conductive\ composites}} \qquad (3)$$

The incorporation of conductive fillers into the elastomeric matrix decreases the Poisson's ratio of the conductive composites below 0.5, generally increasing the total volume of the conductive composites according to the applied strains. Therefore, the volume fraction of conductive fillers in the composites decreases with increasing applied strains. As a result, from the Equation (1), the electrical conductivity of conductive composites decreases with the increasing applied tensile strains.

According to the theoretical models regarding the electrical conductivity of conductive composites, the electrical conductivity can be improved by increasing conductive fillers in the composites, but the high-volume fraction of conductive fillers could degrade the mechanical stretchability of the composites. In general, the conductive composites composed of conductive fillers and elastomeric matrix inherently show the trade-off relationship between the electrical conductivity and stretchability of the composites. Therefore, there is a need for stretchable conductive yarns that exhibit excellent electrical conductivity and high stretchability simultaneously. Lee et al. developed high-performance stretchable conductive yarns via a chemical reduction process using AgNPs and commercial spandex fibers (Figure 4i).[24] A large number of AgNPs were incorporated into commercial elastic yarns comprising a multifilament structure by repeating the chemical reduction process, thus yielding stretchable conductive fibers. The AgNPs were gradually distributed inside the fiber because of the gradual absorption of Ag precursors toward the center of the yarn during the absorption step of the Ag precursors, resulting in the formation of a Ag-rich shell along the surface of the yarn. This Ag-rich shell on the multifilament structure was cracked during stretching, thus effectively retaining the electrical pathways of electrons under high tensile strain (Figure 4j). Based on the synergic effect of the multifilament structure and Ag-rich shell of the yarn, stretchable conductive yarns with simultaneous outstanding electrical stretchability and excellent electrical conductivity were fabricated (Figure 4k). The proposed approach to fabricate stretchable conductive yarns by the chemical reducing reaction has a strong potential for industrial applications, as it is applicable for commercial yarns, already verified in the industry.

## 3.3. Structural Approaches for Fabricating 1D Stretchable Electrodes

Various stretchable conductive yarns based on incorporating or coating conductive materials provide high electrical conductivity and intrinsic stretchability; however, their electrical conductivities generally change during stretching because of the loss of contact between the conductive materials. The change in the electrical properties of these yarns with the applied strain make them a promising candidate as a wearable sensing device; however, if these yarns are used as fiber electrode or an interconnection within electronic devices, the devices may suffer severe performance degradation. To avoid the degradation of the electrical conductivity of the yarn during stretching, various structural designs such as twisted, helical, buckling, and winding structure have been explored for 1D stretchable electrode.[49,94–104] Because the structured yarns dominantly use the deformation of their structures rather than intrinsic stretching of the yarns, the contacts between conductive materials in the yarns can be effectively maintained, in turn minimizing the change in the electrical conductivity of the yarns during stretching.

Shang et al. designed stretchable spring-like CNT ropes by over-twisting a yarn composed of randomly oriented SWCNTs (**Figure 5**a and b).[105] The fabricated CNT ropes provided a high mechanical stretchability under a strain of up to 285% strains and maintained high and stable electrical conductivity during stretching. This was possible because of the loop opening and straightening of the spring structure. The electrical resistance of the yarn was reproducibly increased with only 2% under 20% strains and 11% under 40% strains. In a similar manner, Zhang et al. developed a 1D stretchable electrode by designing freestanding springs composed of aligned MWCNTs (Figure 5c).[100] The freestanding spring-like electrode was fabricated by overtwisting an aligned MWCNT sheet. The fabricated spring-like electrode exhibited a high stretchability of over 300%. The structure of aligned CNTs in the 1D electrodes could also be almost remained under strain because most applied strains were compensated for by the deformation of the spring structure. The electrical resistance of the 1D electrode increased slightly from 0.19 to 0.25 $\Omega$ cm$^{-1}$ under high tensile strains of up to 100%, and then recovered to 0.20 $\Omega$ cm$^{-1}$ after releasing (Figure 5d). Xu et al. used a freestanding spring-like Zn wire as a 1D stretchable electrode for fiber energy devices.[106] Despite the intrinsic rigidity of the Zn wire, the spring structure endowed the 1D electrodes with stretchability, demonstrating that spring-like electrodes can be applied as stretchable electrodes for a 1D stretchable Zn–air battery.

One of other approaches to use structural design for 1D stretchable electrode is to wind conductive wires around an elastomeric wire substrate. He et al. designed a 1D stretchable electrode by convolving the Cu microwire on an elastic silicone rubber wire (Figure 5e).[107] As the shape deformation of the core elastic wire substrate was much higher than that of the convolved Cu wire, the core wire substrate began separating from the Cu wire during the stretching of the 1D system, thereby straightening the convolved Cu wire (Figure 5f). The advanced structural design allows the 1D system to be stretched up to strains of 70% and maintains the electrical conductivity of
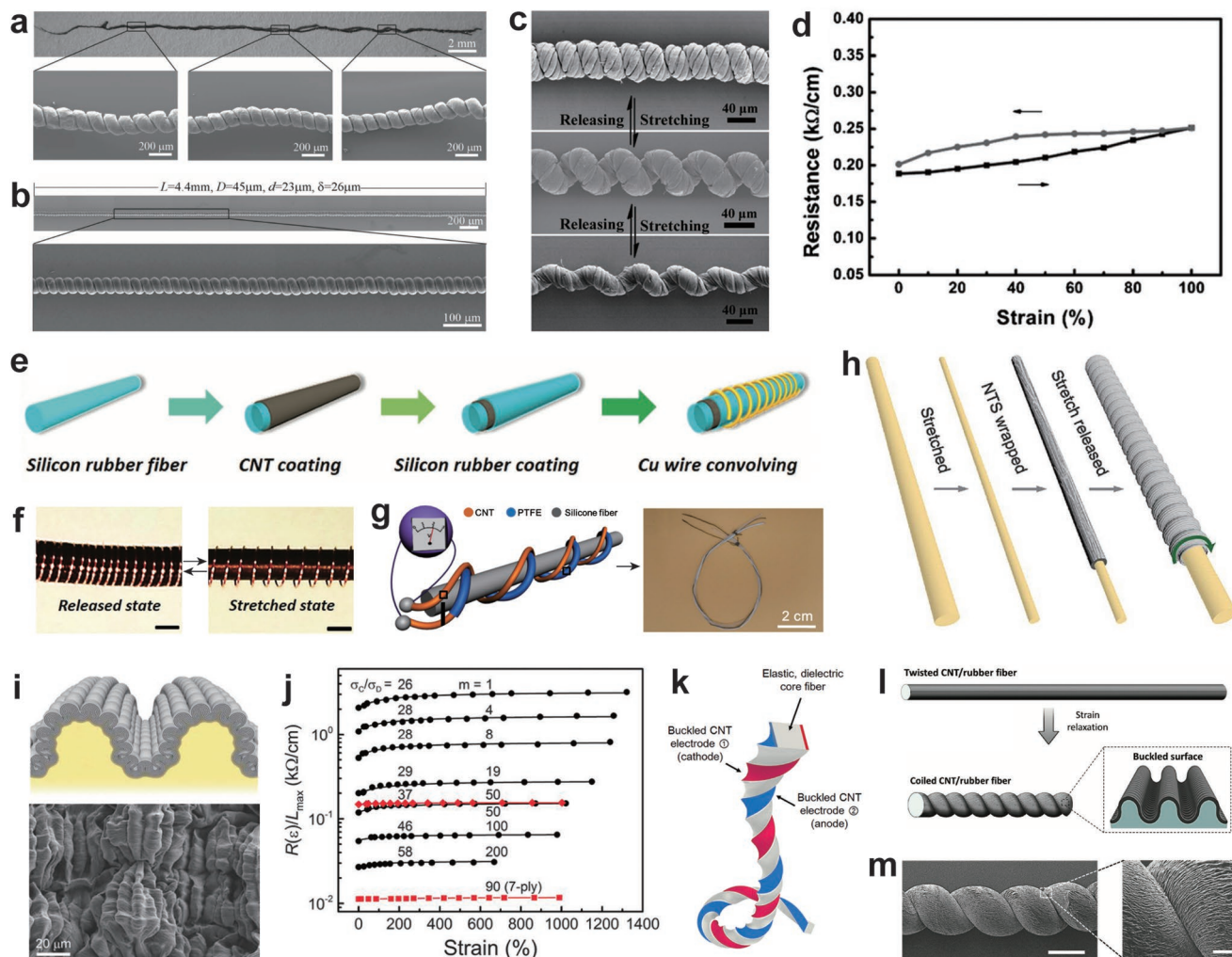
**Figure 5.** a) Photograph of a 3 cm long as-spun CNTs-based stretchable conductive fibers in naturally relaxed state and its corresponding higher-magnification SEM images show the loop structure in corresponding places. b) SEM images of a 4.4 mm long section of rope consisting of highly uniform, perfectly arranged loops and the corresponding higher-magnification image. (a,b) Reproduced with permission.[105] Copyright 2012, Wiley-VCH. c) SEM images of the CNTs-based spring-like stretchable conductive fiber at different strains of 0%, 50%, and 100%. d) Electrical resistances of the stretchable conductive fiber during the stretching and releasing process with a strain of 100%. (c,d) Reproduced with permission.[100] Copyright 2014, Wiley-VCH. e) Schematic illustration of the stretchable fiber nanogenerator based on helically wound fiber electrodes. f) Photographs of the helically wound Cu wire electrode at released state and stretched state. (e,f) Reproduced with permission.[107] Copyright 2016, Wiley-VCH. g) Schematic illustration of the coil structure of CNT-coated cotton thread in stretchable fiber electrodes in fiber energy harvesting devices (left). The photograph of the fabricated fiber devices with curved shape (right). Reproduced with permission.[108] Copyright 2015, Wiley-VCH. h) Schematic illustration of the fabrication of the stretchable conductive fiber based on the buckled structure of MWCNT layers. i) Schematic illustration and SEM image showing the surface of the stretchable conductive fiber based on the 2D hierarchical buckling of MWCNT layers. j) The resistive response of the stretchable conductive fiber based on the buckled MWCNT electrode according to the applied strains. (h–j) Reproduced with permission.[99] Copyright 2015, Science. k) Schematic illustration of the twist-inserted rectangular sandwich fiber, which comprises an Ecoflex rubber core and two symmetric, buckled CNT electrodes. Reproduced with permission.[98] Copyright 2016, American Chemical Society. l,m) Schematic illustration and SEM images showing the stretchable conductive fiber based on the twisted structure and 2D hierarchical buckling of MWCNT layers. Reproduced with permission.[97] Copyright 2016, Wiley-VCH.

the Cu wire during the stretching. Similarly, Zhong et al. used the coil structure of CNT-coated cotton thread in 1D stretchable electrodes in 1D energy harvesting devices (Figure 5g).[108] The CNT-based conductive thread was coiled around a stretchable silicone wire substrate to form a helical structure. The fabricated 1D system could be stretched up to 25% based on the helical structure while maintaining the electrical property of the conductive thread electrode. These structural designs are mainly used for 1D electrodes in 1D stretchable energy devices

wherein the overall device performance strongly depends on the electrical conductivity. More details of the structural designs for 1D electrodes will be further discussed in a later section on stretchable fiber energy devices.

Meanwhile, highly stretchable conductive yarns that can be intrinsically stretched and can effectively retain their electrical conductivity have been developed by applying a structural design to conductive materials coated on an elastic wire substrate. In particular, the buckling structure of conductive

materials in stretchable conductive yarns can provide excellent stretchability without obvious degradation of electrical conductivity.[97–99] Liu et al. developed highly stretchable core-sheath conductive yarns by creating buckled CNTs sheets on elastic wire substrate (Figure 5h).[99] The periodic hierarchical buckling structure of CNTs sheets was realized by wrapping a MWCNT sheath on a prestretched rubber wire core (Figure 5i). The resulting stretchable conductive yarn exhibited outstanding performance in that its electrical resistance changed by less than 5% even under 1000% stretching (Figure 5j). Furthermore, the strain range within which the electrical conductivity of the yarn was maintained almost constant could be increased by coiling the yarn on a core wire substrate. The resistance of the coiled yarn reversibly changed by only 5% under a tensile strain of 3000%. The highly stretchable conductive yarns based on the hierarchically buckled CNTs sheets too have been applied in sandwiched and twisted structures for high-performance 1D stretchable electrodes or interconnects in 1D wearable sensors and energy devices (Figure 5k–m).[97,98]

## 4. 1D Stretchable Electronic Devices and Applications

Owing to the unique structural features of 1D stretchable conductive yarns, they have been effectively applied to realize various 1D electronic devices for advanced wearable electronics and textile electronics. The 1D electronic devices offer an outstanding suitability to be applied to 1D or 3D complex structures compared to most existing 2D planar devices. The superior suitability enables the 1D electronic devices to overcome the practical limitations of the previous electronic devices in wearable electronics. In particular, the property of weavability of the 1D electronic devices is a leading remarkable development in the fields of smart textiles and textile electronics. In this section, we will discuss representative electronic devices based on 1D stretchable conductive yarns and their various applications.

### 4.1. 1D Stretchable Strain Sensors

To date, some of the typical 1D stretchable electronic devices are mechanical sensors that measure a strain, pressure, bending, torsion sensor, and so on. Among these, because of the simplicity of sensor design, various strain sensors based on 1D stretchable electrodes have been developed.[109,110] In particular, most existing 1D stretchable electrodes themselves that are made by the coating or percolation of conductive materials in an elastomeric matrix can be readily used as a resistive strain sensor by means of the strain-dependent changes in their electrical conductivity. In addition, a great demand for high-performance strain sensors for movement and for biomechanical signal monitoring in various fields has further promoted the development of 1D strain sensors.

Eom et al. developed a 1D strain sensor by the in situ polymerization of conducting polymers on yarns (**Figure 6**a,b).[111] The conducting polymer, poly(3,4-ethylenedioxythiophene) (PEDOT), was directly polymerized on the surface of a PE yarn, showing the initial electrical resistance of ≈600 Ω cm$^{-1}$. In order to demonstrate the sensors for wearable applications, the fabricated 1D strain sensors were integrated into a commercially available fabric with two types of patterns (linear and zigzag) by a typical sewing method. The textile strain sensor exhibited a strain gauge factor (GF) over 0.76 with the applied tensile strains of 20%, demonstrating its potential for various wearable applications such as smart gloves. In general, the performance of resistive strain sensors based on organic or inorganic nanomaterials, indicated by parameters such as GF and stretchability, mainly depends on the contacts between the nanomaterials as these contacts decide the conductive paths in the sensors.[112] For achieving high GF, the electrical contacts between conductive materials in the sensors should be sensitively broken and restored against the applied tensile strains, leading to low stretchability of the sensor. Therefore, it is generally difficult to achieve high sensitivity (i.e., high GF) and broad strain-sensing range (stretchability) simultaneously. According to the 3D percolation theory which can explain the electrical behavior of conductive composites under tensile strains, the use of high-aspect-ratio materials such as CNTs and NWs as a conductive material for conductive composite can improve the stretchability of the conductive composites. Cao et al. fabricated presented a 1D strain sensor using AgNWs and a PU composite with a core-sheath structure (Figure 6c,d).[60] The 1D strain sensor was fabricated by coating the AgNWs/PU composite on the surface of an elastomeric core wire, providing an initial electrical resistance less than 1 Ω cm$^{-1}$. Owing to the high-aspect-ratio of AgNWs, the 1D sensor exhibited a large strain sensing range of 60%, as well as a high GF of up to 9557, and a low strain detection limit of 0.1%. In particular, an interfacial bonding layer was additionally introduced between the elastomeric core wire and the AgNWs/PU conductive composite to modulate the stretchability and GF of the 1D sensor. For further increasing the theoretically limited stretchability of the 1D strain sensors by using the conductive composite, metallic NWs were combined with NPs in the 1D elastomeric matrix.[61] The strain sensing range of the 1D strain sensor composed of AgNWs and AgNPs in the elastomeric filament increased to 220% based on the bridging effect of the aligned AgNWs for the AgNPs network under tensile strains (Figure 6e). This high-performance 1D strain sensor was successfully applied for developing an artificial smart glove to detect sign language (Figure 6f–h). Despite the high stretchability of the 1D sensor using the NWs, the synthesis process of the high-aspect-ratio materials is complicated and cost is quite expensive, hindering their use in industry. In this regard, Lee et al. developed a facile approach for fabricating highly sensitive and stretchable 1D strain sensors without any high-aspect-ratio conductive fillers (Figure 6i–k).[24] The developed 1D strain sensor was fabricated by incorporating only AgNPs into multifilament-structured elastomeric filaments through a simple chemical reduction process. The conductive paths in the 1D sensor could be exceptionally maintained under high tensile strains based on its Ag-rich layer and multifilament structure, yielding high performance. Although no high-aspect-ratio conductive fillers were included in the sensor, the fabricated sensor achieved outstanding sensitivity to tensile strain (≈9.3 × 10$^5$ and ≈ 659 in the first stretching and subsequent stretching, respectively) along
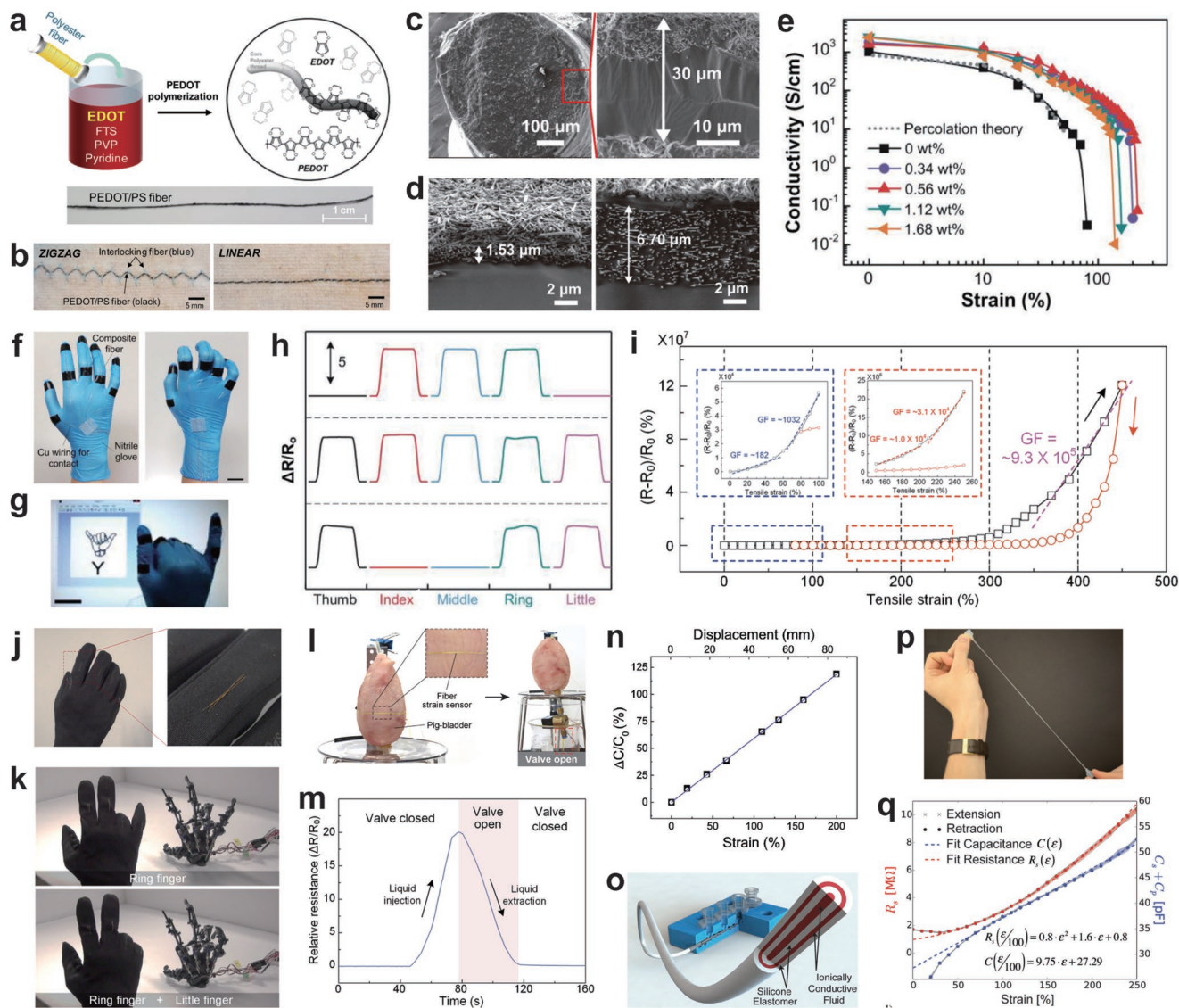
**Figure 6.** a) Schematic illustration of polymerization of PEDOT on a PS fiber. b) Optical images of linear- and zigzag-type stretchable conductive fiber-embedded fabrics. c) SEM images of the cross section of the AgNWs/PU-based stretchable conductive fiber. d) Cross-sectional SEM images of the AgNWs/PU fibers with different prepolymerization time of 20 min (left) and 15 min (right). (a–d) Reproduced with permission.[111] Copyright 2017, American Chemical Society. e) Conductivity change of stretchable conductive fiber fabricated with the AgNWs and AgNPs with respect to increasing strains. f) Photograph of the smart glove developed using the stretchable conductive fiber with AgNW-AgNP composite. Scale bar is 2 cm. g) Photograph of detecting English letter "Y" with the smart glove. h) Finger motion detection in the smart glove. (e–h) Reproduced with permission.[61] Copyright 2015, Wiley-VCH. i) Relative change in the electrical resistance of the multifilament fiber-based fiber strain sensor as a function of the first applied and released maximal strain. Inset graphs show the strain range of 0–100% and 150–250%, respectively. j) Photograph of the smart glove based on the fiber-based strain sensors on the nodes of the five fingers. k) Photographs of a remotely operated hand robot controlled by the smart glove. l) Photograph of the artificial bladder system and its operation with the fiber-based strain sensor on the pig bladder. m) Resistive response of the fiber-based strain sensor on the pig bladder and the operation of a solenoid valve according to the injection and extraction of liquid. (i–m) Reproduced with permission.[24] Copyright 2018, American Chemical Society. n) The dependence of CNT conductive fiber-based strain sensor's capacitance on strain and displacement during stretching and stretch release, where the blue line is a linear fit of the data. Reproduced with permission.[114] Copyright 2016, Wiley-VCH. o) Schematic illustration of multicore-shell printing process for capacitive soft strain sensor fibers. p) Photograph of the stretched capacitive fiber strain sensor. q) Model predictions, sensor resistance, and total capacitance of the capacitive fiber strain sensor up to 250% strain. (o–q) Reproduced with permission.[113] Copyright 2015, Wiley-VCH.

with a largely wide strain sensing range (450 and 200% for the first and subsequent stretching, respectively) at the same time (Figure 6i). This 1D strain sensor was integrated into knuckles of a glove using a typical sewing method, demonstrating that the 1D sensor could be used to detect human motions precisely

and to control robot movements according to the recognized human motions (Figure 6j,k). In addition, the potential of the developed 1D strain sensor in biomedical applications has been demonstrated. An artificial bladder system, which can monitor the volume expansion of a bladder in real time and control

**ADVANCED
SCIENCE NEWS**

www.advancedsciencenews.com

**ADVANCED
MATERIALS**

www.advmat.de

the extraction of the liquid in the bladder, was developed by applying the 1D strain sensor onto a 3D curved surface of a porcine bladder (Figure 6l,m). The 1D strain sensor successfully detected the strain on the bladder surface generated from the volume expansion of the bladder and a solenoid valve connected to the outlet of the bladder was controlled according to the sensor response. Thus, the ability of the artificial bladder system equipped with the 1D strain sensor to effectively regulate its volume was demonstrated.

In addition to resistive 1D strain sensors, capacitive-type 1D strain sensors have also been investigated considering their advantages in terms of high stability, low hysteresis, and low power consumption.[99,113,114] In general, capacitive sensors consist of a dielectric layer, which can be deformed in response to the applied deformation, sandwiched between two electrode layers. Wang et al. presented a capacitive 1D strain sensor with high stretchability fabricated by coating a coaxial, alternating layers of hierarchically buckled CNT layers and an insulating rubber layer on an elastomeric fiber substrate.[114] Especially, mechanical interference during the stretching of the 1D sensor was minimized by downsizing the whole diameter to 160 µm, leading the mechanical stretchability of the 1D sensor. The developed 1D sensor provided a 119% linear increase in capacitance during stretching up to 200% strain, without obvious hysteresis (Figure 6n). In addition, the high stability of the sensor over thousands of stretching cycles and high sensitivity to small changes in strain of below 1% were investigated, and these properties were largely attributed to the downsized structure and highly stretchable buckled CNT electrodes. Using the coaxial structure, Lewis and co-workers also developed a capacitive 1D strain sensor by a microfluidics-based multicore-shell fiber printing approach (Figure 6o–q).[113] The designed 1D strain sensor consists of four coaxial, alternating layers of a conductive liquid and a silicon elastomer, in which capacitance is created between two coaxial conductive liquid layers. The capacitive response of the sensor, which is mainly determined by the length of fiber and geometrical parameters of the coaxial structure, was reliably measured up to high tensile strains of 250% with high accuracy and negligible hysteresis under both static and dynamic operating conditions. In addition, it was demonstrated that the capacitive 1D strain sensor could be readily integrated into textiles for wearable electronics, human/machine interfaces, and smart textiles.

### 4.2. 1D Stretchable Pressure, Bending, and Torsion Sensors

Technically, various 1D strain sensors also respond to other mechanical deformations such as pressure, bending, and torsional stimulations because the mechanical deformations are closely related each other. These mechanical deformations are not only more complicated than linear strain deformation, but also significantly important in practical applications in which the deformations are commonly observed, for example, in the study of the movement of joints and muscles. Therefore, many attempts have been carried out to design stretchable 1D mechanical sensors that can detect various mechanical deformations.[49,58,63,115–123] Cheng et al. developed a stretchable and sensitive graphene-based 1D mechanical sensor by coating

rGO onto the surface of yarns with a compressed spring structure (**Figure 7**a).[49] The compressed spring structure of the 1D sensor generated gaps between microstructure of the wound yarns and induced sensitive change in the contact area between the yarns, providing high sensitivity to various mechanical deformations such as strain, bending, and torsion. The 1D sensor revealed a wide sensing range of bending angle up to 90°, high sensitivity with a small detection limit of 2°, and stable repeatable response in forward and reverse directions (Figure 7b). In addition, a wide dynamic torsion-sensing range from −280 to 800 rad m$^{-1}$ (Figure 7c), a low torsion detection limit of 2 rad m$^{-1}$, and high stability over 5000 cycles of torsional deformation were realized. The developed 1D mechanical sensor was successfully used as a wearable sensor, demonstrating the detection of full-range human activities such as subtle speech recognition, sleep quality evaluation, pulse monitoring, and various human motions. Chen et al. reported a highly stretchable 1D mechanical sensor fabricated by coating P(VDF-TrFE) polymeric nanofiber mats and AgNW layers onto an elastomeric fiber substrate.[58] Based on the AgNW network layers, the fabricated sensor showed sensing abilities for various mechanical stimuli such as bending, torsion, and tensile strain. As a bending sensor, it had a broad bending-angle sensing range up to 130°, a low minimum bending-angle detection limit of 1.5°, and negligible hysteresis (Figure 7d). Simultaneously, the 1D sensor provided an outstanding broad range of torsion sensing up to 6000 rad m$^{-1}$. In addition to the bending and torsional deformations, a stretchable piezoresistive 1D pressure sensor was developed by simply twisting two stretchable conductive yarns (Figure 7e).[117] The stretchable yarn electrode comprised durable core-shell conductive yarns with a high conductivity of 10$^{-4}$–10$^{-5}$ Ω cm and stretchability of ≈400%; these conductive yarns were fabricated using multiscale wrinkled microstructures of AgNW/PU composite. The stretchable piezoresistive 1D pressure sensor was fabricated by twisting the two yarn electrodes (Figure 7e). The change in contact area between the wrinkled microstructured surfaces of the two yarn electrodes in the sensor offered a desirable sensitivity of 0.12 kPa$^{-1}$, a fast response and relaxation time (35 and 15 ms), a low detection limit of 10 mg, and an excellent working stability for more than 4000 loading/unloading cycles against external pressure stimuli. In addition, the 1D sensor also exhibited a high sensitivity of 0.012 rad$^{-1}$ to bending deformation because these deformations produced local stress on the 1D sensor. Similarly, Cooper et al. presented a soft and stretchable capacitive 1D sensor for torsion, touch, and strain by intertwining two core–shell conductive filament yarns composed of an elastomeric polymer fiber shell filled with conductive liquid metal (EGaIn) (Figure 7g).[118] The torsional deformation of the 1D sensor induced an increase in the contact area between the two twisted conductive yarns and thus changes the capacitance between the two yarns, providing the ability to detect changes in torsion up to 10 887 rad m$^{-1}$ (Figure 7h). This wide sensing range of the sensor was two orders of magnitude higher than that of the previously reported torsion sensors at that time. Although 1D mechanical sensors can sensitively detect various mechanical deformations such as pressure, bending, torsion, and strain, all the sensing modes generally depends on same output value of the sensor.
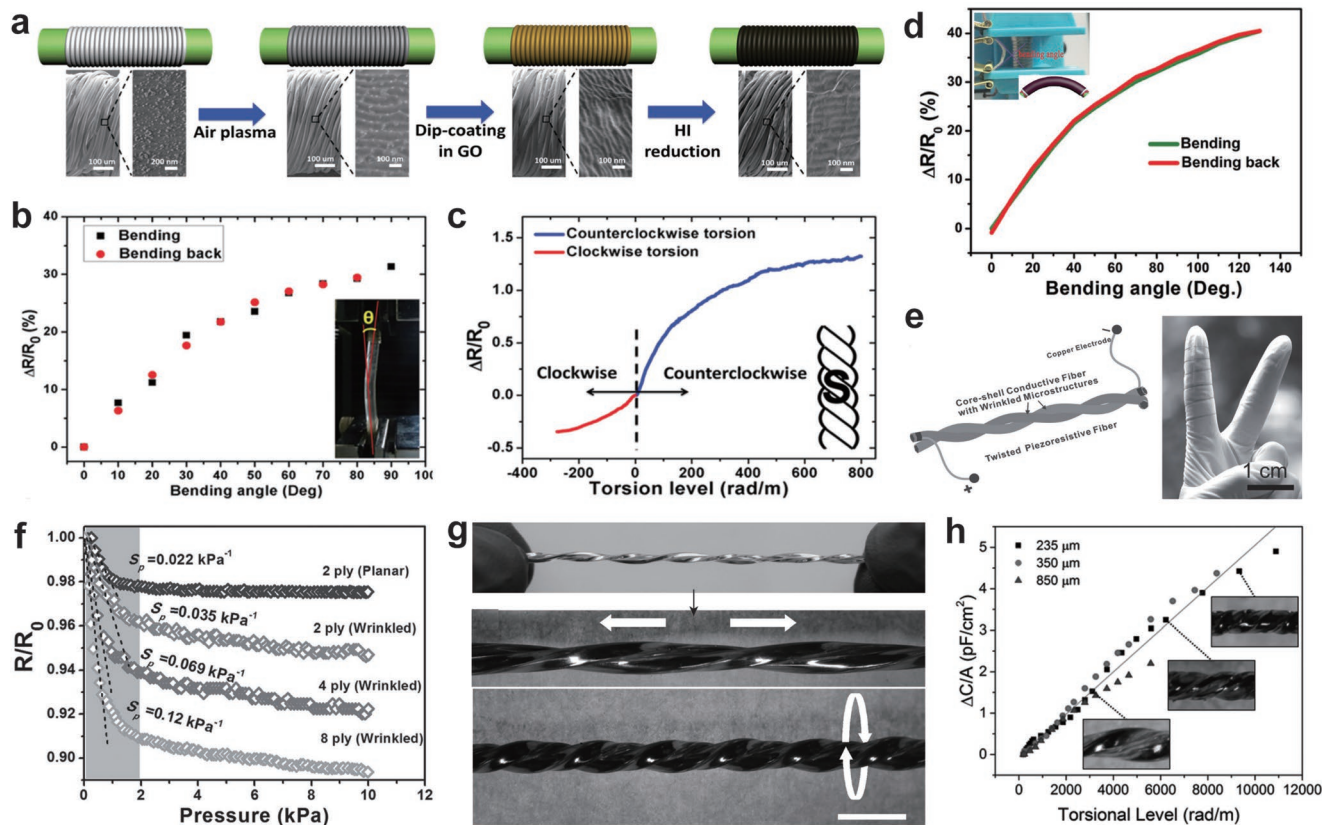
**ADVANCED
SCIENCE NEWS**
www.advancedsciencenews.com

**ADVANCED
MATERIALS**
www.advmat.de

**Figure 7.** a) Schematic illustration of the fabrication process of stretchable and sensitive graphene-based fiber mechanical sensor. b) Resistance variation of the fiber-based mechanical sensor in forward bending and reverse bending. Inset: Photograph of the bending sensor in testing. c) Resistive response of the graphene-based mechanical fiber in torsion test from −280 to 800 rad m$^{-1}$. (a–c) Reproduced with permission.[49] Copyright 2015, Wiley-VCH. d) Resistive response of the stretchable conductive fiber-based mechanical sensor in forward and backward bending. Reproduced with permission.[58] Copyright 2016, Wiley-VCH. e) Schematic illustration and photograph of the stretchable piezoresistive fiber pressure sensor. f) Relative resistance change of different piezoresistive fibers according to the applied pressure. (e,f) Reproduced with permission.[117] Copyright 2016, Wiley-VCH. g) Photograph of two twisted liquid metal core fibers with 850 µm diameter (top), stretched up to 150% strain (middle), and additional twisting with torsional level to 1260 rad m$^{-1}$ (bottom). Scale bar is 2.5 mm. h) Capacitance change of the stretchable fiber torsion sensor according to the applied torsional deformations. (g,h) Reproduced with permission.[118] Copyright 2017, Wiley-VCH.

Therefore, at present, it is difficult to decouple the applied mechanical deformations from the output signal, hindering its practical application in real life. Future work on mechanical sensors for various deformations should focus on decoupling the different deformations applied simultaneously.

### 4.3. 1D Stretchable Thermal Devices for Wearable Applications

One of the newly emerging wearable devices is a wearable heater which can help human body maintain a safe temperature in extreme environments such as high mountains and Antarctic bases. Because it is most efficient for the wearable heaters to be integrated into clothes that are essential in extreme environments, 1D wearable heaters have been actively developed using various electrothermal materials such as CNTs, graphene, and metallic nanomaterials for smart textile and wearable applications.[24,50,63] The electrothermal efficiency and power consumption mainly depends on the electrical conductivity of the electrothermal electrode in the heater. Therefore, the electrical properties of the 1D conductive electrode

are the key parameter for the fiber heater. In addition, because the wearable heater that typically covers human motion is inevitably affected by external mechanical deformations such as stretching and bending, its stretchability and the electrical conductivity determine the heating performance of stretchable 1D heating devices. Sun and co-workers presented a wearable heater fabricating using 1D stretchable conductive electrodes with a hierarchical structure (**Figure 8**a).[63] The 1D stretchable heater was fabricated using CuNW-based 1D conductive composite, and it could be heated from 20 to 57 °C at an acceptable DC voltage of 3 V with a fast response time under 20 s (Figure 8b). Based on its high stretchability, stable electrical conductivity can be maintained under various deformations such as bending, twisting, and stretching. Hence, the heating performance of the 1D stretchable heater revealed no any clear degradation after various mechanical deformations. The 1D stretchable heater could be readily woven into textiles, successfully demonstrating its potential for practical applications as a wearable textile heater for articular thermotherapy and maintaining the body temperature of infant models (Figure 8c). Wang et al. developed 1D graphene based heaters with high
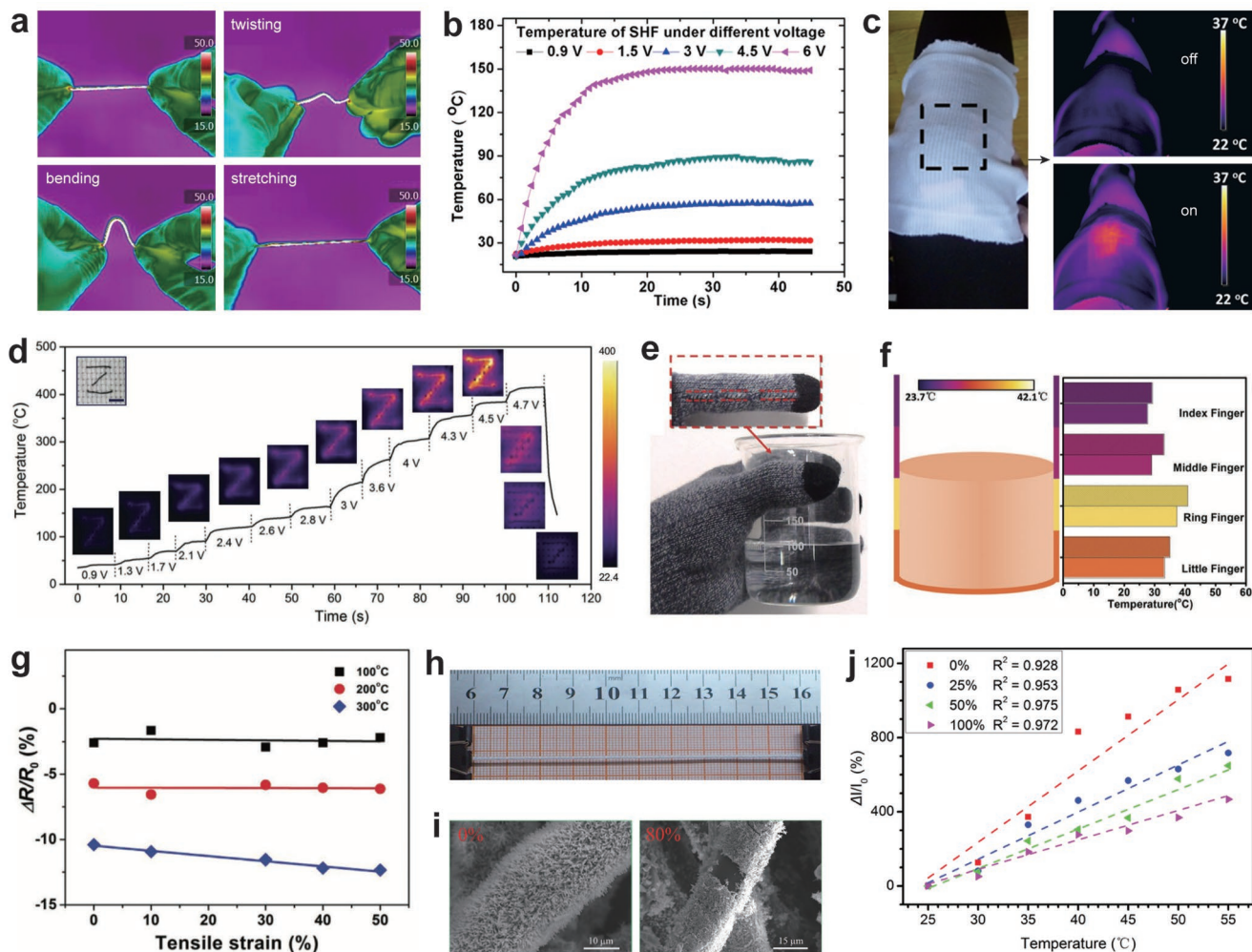
**Figure 8.** a) IR thermal images of stretchable heating fiber at original state, twisting state, bending state, and stretching (strain of 50%) state under constant voltage of 1.2 V. b) Time-dependent temperature curves of stretchable heating fiber under different constant dc voltages from 0.9 to 6 V. c) Photograph of wearable and smart personal heating system application at the knee position of a human body (left) and IR thermal images before and after switching on the device (right). (a–c) Reproduced with permission.[63] Copyright 2016, American Chemical Society. d) Temperature profiles of Z-patterned graphene fiber heater under stepwise voltage from 0.9 to 4.7 V. Inset: optical and thermal images of Z-pattern fabric. Reproduced with permission.[50] Copyright 2016, Wiley-VCH. e) Photograph of a particular glove weaved with the fiber thermal sensor on four fingerstalls except thumb, sensor, on index finger is highlighted with red mark. f) The corresponding temperature distribution detected by glove thermal sensor and the right histograms are exact temperature values measured by an infrared camera (oblique line) and stretchable fiber thermal sensors (blank), respectively. (e,f) Reproduced with permission.[124] Copyright 2016, Wiley-VCH. g) Resistance change in the same helical rGO stretchable fiber stretched to strain of 0–50% and heated to temperatures of 100, 200, and 300 °C, respectively. Reproduced with permission.[125] Copyright 2016, Royal Society of Chemistry. h) Photograph of the elongated ZnO NWs-based stretchable fiber sensor. i) SEM images of the stretchable fiber-based sensor under 0% and 80% strain. j) Normalized current changes of the stretchable fiber temperature sensor versus temperature under 0%, 25%, 50%, and 100% strain. (h–j) Reproduced with permission.[126] Copyright 2016, Wiley-VCH.

stretchability, ultrafast electrothermal response and low operation voltage by twist-spinning thermally treated graphene conductive films.[50] Through the thermal treatment of the graphene films which could heal the structural defects in the graphene. Thus, the electrical conductivity of the stretchable graphene yarn was greatly improved to $6 \times 10^5$ S m$^{-1}$. Owing to the high electrical performance of the yarn, the graphene yarn-based heater exhibited high heating performance. The 1D heater could reach high temperatures up to 424 °C at a low input voltage of 5 V with ultrafast electrothermal response of heating rate 571 °C s$^{-1}$ and cooling rate 891 °C s$^{-1}$ (Figure 8d). It was effectively integrated into applicable electrothermal

fabrics, and stable heating performance was achieved during the motion of the human finger and wrist.

1D stretchable conductive electrodes have also been applied to develop wearable temperature sensors for practical applications.[124–126] He et al. developed an 1D stretchable thermal sensor using organic semiconducting materials (Figure 8e,f).[124] Through a simple, continuous dyeing process, polypyrrole was coated on the surface of normal Dacron threads, which were subsequently wound into a coiled structure. Because of the semiconducting properties of the coated polypyrrole, the fabricated 1D electrode obtained higher conductivity when the environmental temperature rose, enabling the electrode to act as a

1D wearable thermal sensor. In particular, the 1D sensor exhibited the conductivity change of 5.37% with the temperature change of 10 °C (from 25 to 35 °C) and high stability under severe bending or tensile strain based on its coiled structure. In addition, based on the photothermal conversion ability of polypyrrole, the 1D sensor could also detect near-infrared (NIR) irradiation by means of the thermal excitation effect. It was demonstrated that the fabricated 1D sensor could be directly used to develop wearable smart gloves which can monitor the environmental temperature. Similarly, Hua et al. used an 1D rGO-based helical stretchable electrode as a stretchable yarn-based temperature sensor for wearable application.[125] The stretchable conductive yarn was fabricated by directly spinning freestanding GO films into helical structures. The semiconductor behavior dominated by carrier hopping among the stacked rGO sheets in the fabricated 1D electrode offered the temperature sensing ability to the stretchable yarn. The 1D stretchable temperature sensor exhibited a reliable deformation-independent response for high temperatures up to 300 °C under high strains of 50% (Figure 8g).

Liao et al. developed an 1D stretchable temperature sensor by using pyroelectric materials in an 1D stretchable sensor (Figure 8h–j).[126] The 1D stretchable sensor was prepared by growing ZnO NWs on stretchable PU filaments. Owing to the pyroelectonic effect of the ZnO NWs, the elevated temperatures induced spontaneous polarization and charge separation in the ZnO NWs, providing the increase in the current in the filament and thus the temperature sensing ability. The 1D stretchable temperature sensor exhibited a high sensitivity of up to 39.3% °C$^{-1}$. In addition, the 1D stretchable sensor showed the ability to detect UV light based on oxygen adsorption and desorption on the ZnO NWs under UV illumination.

### 4.4. 1D Stretchable Energy Storage Devices

High-performance 1D energy devices has been recognized and developed as a promising strategy to overcome the limitations of previous energy devices in wearable applications due to its high flexibility and suitability to be integrated into other textile products through conventional weaving or sawing techniques.[1,4,5] For fabricating such 1D energy devices, metallic wires or conducting polymer-based wires have been conventionally investigated as 1D electrodes of the devices; however, their inherent poor stability against external deformations, poor electrochemical activities, and relatively small surface areas have limited the advancement of 1D energy devices for wearable electronics.[127–131] In this regard, carbon nanomaterial-based 1D electrodes assembled from CNTs, graphene, or their composites have been mainly investigated to replace the conventional wire electrodes based on their high mechanical, electrical, electrochemical properties, and large specific surface areas which enhance their electrochemical properties (**Figure 9**a).[1,5,132–135]

Based on the carbon nanomaterial-based fiber electronics, at present, a variety of 1D energy storage devices such as supercapacitors,[136–146] lithium-ion batteries,[100,147–151] lithium–sulfur batteries,[152] lithium–air batteries,[153] and zinc–air batteries[106] have been developed. In particular, 1D stretchable supercapacitors, which will be mainly outlined in this review article, have gained considerable interest as an energy storage device due to their high-power density, short charging time and long cycling life.[1,4] The performance of the stretchable energy devices largely depends on the electrical performance of its electrode under applied tensile strains. To achieve 1D stretchable supercapacitors that have stable electrochemical performance under external tensile strain, the high electrical conductivity of the electrode too should be maintained. For this purpose, functional materials and electrodes are typically introduced onto elastic fiber substrates in various ways. Yang et al. developed stretchable fiber-shaped supercapacitors with coaxial structures by layer-by-layer coating of an aligned CNT layer, gel electrolyte and a shell CNT layer onto an elastic rubber fiber (Figure 9b,c).[154] The developed 1D stretchable supercapacitors maintained its structure and high specific capacitance of 18 F/g even after a tensile stretching of 75% for 100 cycles. The coaxial stretchable 1D supercapacitor based on the aligned CNT layer was further improved by wrapping the aligned CNTs/polyaniline (PANI) composite sheets on the elastic fiber substrate that are prestretched with a tensile strain of 50%.[155] The electrical performance of the coated aligned CNTs/PANI composite sheets was also improved by adjusting the wrapping helical angles and thickness of the aligned CNTs, providing a low initial resistance of 0.18 kΩ cm$^{-1}$ and a small amount of increase in the resistance according to the applied strain (below 70% increment at strains of around 400%). In addition, no obvious damage in the 1D electrode were observed even after repeated stretching by 400% (Figure 9d). Based on the improved stretchable electrode, the galvanostatic charge–discharge profiles of the devices and the specific capacitances remain almost unchanged under stretching with strains to 400% (Figure 9e). In addition, a high specific capacitance of ≈79.4 F g$^{-1}$ was effectively retained after the repeated large strains of 300% for 5000 cycles and ≈100.8 F g$^{-1}$ after repeated bending deformations for 5000 cycles at a current density of 1 A g$^{-1}$. Although the electrical stretchability of the aligned CNT sheets-based 1D electrode was improved for stretchable 1D supercapacitors, it still has the inherent degradation of its electrical conductivity under an applied tensile strains, which induces the capacitance degradation of the 1D supercapacitor.[6]

Against the background of the strong demand for stretchable 1D supercapacitors with minimal performance degradation under tensile strains, a range of structural approaches such as twisted,[156–159] wound,[160–162] buckled,[156,163,164] and spring-like structures[51,165–171] have been applied to improve the electrical stretchability of the electrode, and thus, enhance the stretchable 1D supercapacitors. Chen et al. developed stretchable 1D supercapacitors by twisting two elastic 1D electrodes precoated with an electrolyte and a separator.[157] In order to improve the stretchability of the 1D supercapacitor, the elastic yarn coated with wrinkled CNT sheets, which was fabricated by directly wrapping CNT sheets onto a prestrained elastic fiber substrate with various prestrains, was used as an 1D stretchable electrode. The twisted 1D elastic electrodes in the 1D supercapacitors showed the enhanced electrical stretchability, resulting in an increment of only 30% in its electrical resistance under an external tensile strain of 300%. Based on the presence of these 1D elastic electrodes, 1D supercapacitors exhibited a high
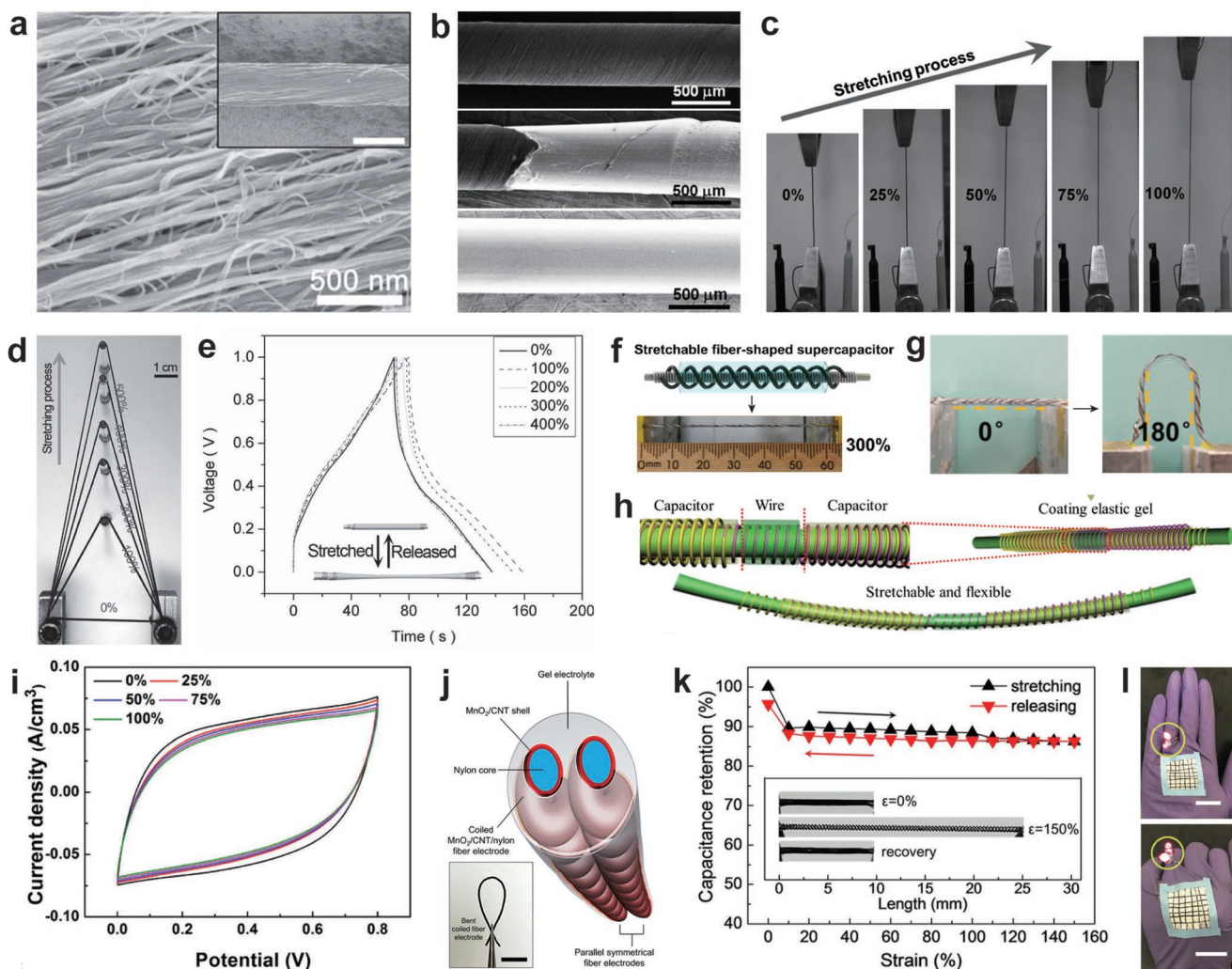
**ADVANCED
SCIENCE NEWS**

www.advancedsciencenews.com

**ADVANCED
MATERIALS**

www.advmat.de

**Figure 9.** a) SEM image of a fiber supercapacitor using CNT/PANI composite fiber. Scale bar of the inset is 50 µm. Reproduced with permission.[135] Copyright 2015, Wiley-VCH. b) SEM images of the inner CNT electrode on the fiber substrate, the left end side, and middle side of the coaxial fiber supercapacitor. c) Photographs of the coaxial fiber supercapacitor under different strains of 0, 25, 50, 75, and 100%. (b,c) Reproduced with permission.[154] Copyright 2013, Wiley-VCH. d) Photograph of an elastic fiber electrode before and after stretching by 100%, 200%, 300%, 400%, and 500%. e) Galvanostatic charge–discharge profiles of the fiber supercapacitor with increasing strains from 0% to 400%. (d,e) Reproduced with permission.[155] Copyright 2014, Wiley-VCH. f) Schematic illustration of the stretchable fiber supercapacitor based on double helical configuration of fiber electrodes (up) and photograph of the fiber supercapacitor at strains of 300%. g) Photographs of the fiber supercapacitor before and after bending deformation with the angle of 180°. (f,g) Reproduced with permission.[161] Copyright 2018, American Chemical Society. h) Schematic illustration of the stretchable tandem fiber supercapacitors consisting of two cells in series. Reproduced with permission.[160] Copyright 2018, Elsevier. i) Cyclic voltammogram curve of the stretchable fiber supercapacitor before and after stretching up to 100%. Reproduced with permission.[51] Copyright 2017, American Chemical Society. j) Schematic illustration for the complete all–solid–state supercapacitor, which comprises two symmetric coiled $MnO_2$/CNTs/nylon fiber electrodes and a gel electrolyte. The inset: optical image showing a bent $MnO_2$/CNTs/nylon fiber electrode, which is held by tweezers (scale bar = 5 mm). k) Capacitance retention versus applied strain during a stretching-releasing cycle up to 150% strain. The inset: optical images of complete coil supercapacitor before, at, and after 150% strain. (j,k) Reproduced under the terms of the Creative Commmons Attribution 4.0 License.[167] Copyright 2015, Springer Nature. l) Demonstration of a fiber supercapacitor powering two LEDs in the normal and curved states. Scale bars are 2 cm. Reproduced with permission.[166] Copyright 2018, Wiley-VCH.

stretchability of up to 350% tensile strain with a high capacitance of up to 30.7 F g⁻¹. The specific capacitance of the 1D supercapacitance changed very slightly during stretching deformation and remained stable even after 100 stretching cycles under 200% tensile strain. By using the twisted structure, Sun et al. realized a large-scale production process of 1D stretchable supercapacitors by twisting the stretchable 1D electrodes fabricated by using conductive CNTs and electrocapacitive

polypyrrole (PPy) on urethane plastic core spun yarns; thus, they devised a scalable and low-cost fabrication route.[158] The 1D stretchable supercapacitors showed a high specific capacitance of 69 mF cm⁻² and the capacitive performance remained nearly unchanged under tensile strains of 80%.

To further minimize the degradation of the electrical performance of the 1D electrodes under tensile strains and thus improve the stretchability of the 1D supercapacitors, the use

**ADVANCED
SCIENCE NEWS**

www.advancedsciencenews.com

**ADVANCED
MATERIALS**

www.advmat.de

of wound structures in 1D supercapacitors was also explored. 1D electrodes were wound directly onto a core stretchable wire substrate in 1D stretchable supercapacitors, enabling the \ electrodes to be minimally stretched during the stretching of the whole 1D structure. Zhao et al. developed a highly stretchable 1D supercapacitor by winding intrinsically stretchable 1D AuNW/Au film/PANI electrodes in a double helical configuration (Figure 9f,g).[161] The double helically wound yarn electrodes were geometrically optimized by adjusting the winding angles of the wound electrodes to realize the highly stretchable 1D supercapacitor. The specific capacitance of the developed 1D supercapacitor was retained after repeated stretching deformations of 200% for 2000 cycles. Based on the high stretchability, the 1D supercapacitors were directly integrated into a usual glove by a sewing method, with negligible changes in its capacitive performance against normal finger movements. Even though the stretchable performance of 1D supercapacitors can be improved by the winding approach, the stretchability of the wound structure-based 1D supercapacitors largely depends on the dimensions of core wire substrates.[162] In addition to its high flexibility and deformability, conductive yarn electrodes in 1D supercapacitors can also be used simultaneously as electrical interconnect components owing to the advantage of its fibrous structure. Based on these unique features of 1D electrodes, Wang et al. demonstrated a highly stretchable 1D supercapacitor by connecting several 1D supercapacitors each other on an elastic wire substrate.[160] Each stretchable 1D supercapacitor was basically fabricated by winding yarn electrodes onto an elastic wire substrate and several 1D supercapacitors were electrically connected each other in series without using any metal wire interconnect and additional welding connection, finally making the group of symmetric assembled tandem 1D supercapacitors (Figure 9h). The resulting stretchable tandem 1D supercapacitors consisting of 8 serially connected capacitor cells exhibited a high voltage output of 12.8 V, energy density of 41.1 $\mu$W h cm$^{-2}$ at power density of 3520 $\mu$W cm$^{-2}$, and a high stretchability of around 400% without obvious degradation of the specific capacitance. However, due to the inherent behavior of the wound wire structure, it is difficult to achieve high stretchability of the wound electrodes despite using the densely wound fiber electrodes as the diameter of the core wire substrate decreases. In particular, the helically wound fiber electrodes can be stretched without any obvious intrinsic stretching of the electrodes until the helical structure of the 1D electrodes is lost by straightening. Therefore, the stretchability of the 1D supercapacitors based on the wound 1D electrodes largely depends on the diameter of the core wire substrate. These inherent structural properties can potentially limit the applications of 1D supercapacitors because the size of the 1D devices should be considered for application in practical textiles or wearable applications. Furthermore, the helically wound 1D electrodes can be intrinsically stretched to some degree even before the helical structure is straightened under tensile strains because of the core wire substrate, which also induces performance degradation of 1D supercapacitors under tensile strains.[169] In order to overcome the confined deformation imposed by the core wire substrate, various substrate-free stretchable structures have been recently investigated for high-performance 1D stretchable supercapacitors. Shang et al.

developed a substrate-free, stretchable 1D supercapacitor based on a uniformly arranged helical structure.[169] The 1D supercapacitor maintained stable capacitive performance under large stretching deformations up to 150%. Wang et al. used rGO springs as stretchable 1D electrodes for an 1D supercapacitor.[51] The springs could be stretched to high strains of up to 300% with an appropriate design, resulting in high stretchable performance of the 1D supercapacitor (Figure 9i). The spring-shaped 1D supercapacitor was also combined with a stretchable self-healing polymer to obtain a self-healable and 1D stretchable supercapacitor.

Although a variety of 1D stretchable energy storage devices have been extensively developed, realizing high long-term stability of these 1D stretchable energy devices as compared to the previous planar devices still remains a challenge.[1] In general, the use of liquid electrolytes in 1D supercapacitors considerably hinders the achievement of the high stability of the 1D devices due to the absence of an effective long-term encapsulation technique for liquids in an 1D stretchable system. Therefore, solid-state 1D supercapacitors based on stable and environmentally friendly gel electrolytes instead of typical liquid electrolytes have been investigated for developing practical applications. Choi et al. developed an 1D stretchable solid-state supercapacitors by using helically coiled $MnO_2$/CNTs/nylon yarn electrodes and gel electrolyte (Figure 9j,k).[167] These all-gel-state 1D supercapacitors generally can offer the strong and stable mechanical properties, enabling the devices to be effectively applied to wearable and textile applications (Figure 9l).[166] Although the use of the solid-state gel electrolyte can overcome the major drawbacks of conventional liquid electrolytes, the stretchability of these 1D supercapacitors also mainly depends on the structure of 1D electrodes in a manner similar to that for the previous fiber supercapacitors. In solid-state stretchable 1D supercapacitors, spring-shaped configuration is realized after the fabrication process in order to achieve high compressibility and stretchability.[168]

## 4.5. 1D Stretchable Energy-Harvesting Devices

In the similar manner with the 1D energy storage devices, 1D stretchable energy-harvesting devices such as solar cells, nanogenerators, and fuel cells, are generally realized by coating electrodes and active materials on a single fiber substrate in a coaxial structure or by twisting 1D electrodes coated with two active materials.[172–180] However, it has been more difficult to fabricate 1D stretchable energy-harvesting devices compared to 1D stretchable storage devices, although stretchable planar energy harvesting devices have been more extensively developed.[5,181–184] For example, because power conversion efficiency, the key factor in the development of photovoltaic devices, of 1D solar cells is generally lower than that of planar solar cells even if the 1D devices are not stretchable, achieving stretchable 1D solar cells with high performance has remained as a great challenge. In particular, the energy harvesting performance of solar cells is greatly affected by the electrical and electrochemical performance of their electrodes. Therefore, it is not easy to achieve and maintain high performance of 1D solar cells under external tensile strains due to the degradation of electrical performance of the 1D electrodes according
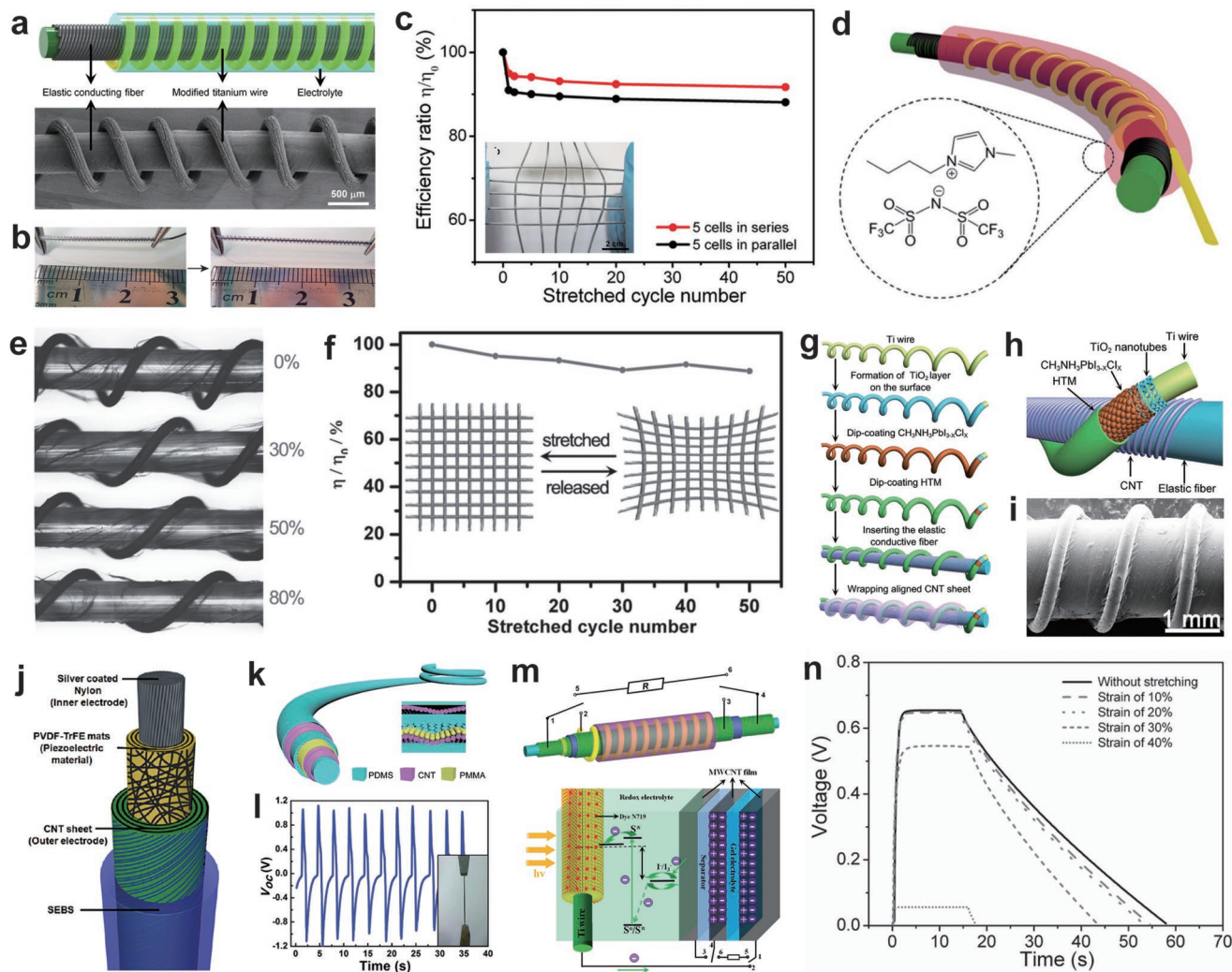
**Figure 10.** a) Schematic illustration and SEM image of the stretchable fiber DSSCs. b) The stretchable fiber DSSCs before and after stretching with a strain of 30%, respectively. c) Energy conversion efficiency of the stretchable fiber DSSC for repeated stretching deformations for 50 cycles at a strain of ≈20%. The inset: photograph of a stretchable photovoltaic textile under the stretching deformation. (a–c) Reproduced with permission.[185] Copyright 2014, Wiley-VCH. d) Schematic illustration to the structure of the stretchable fiber DSSCs based on gel electrolyte. Reproduced with permission.[186] Copyright 2015, Wiley-VCH. e) Photographs of the stretchable fiber polymer solar cell with increasing strain from 0% to 80%. f) Energy conversion efficiency of the stretchable energy textile including the fiber polymer solar cells according to the repeated stretching cycle. (e,f) Reproduced with permission.[187] Copyright 2014, Wiley-VCH. g,h) Schematic illustration of the fabrication process and structure of the stretchable fiber perovskite solar cell, respectively. i) SEM image showing the structure of fabricated stretchable fiber perovskite solar cell. (g–i) Reproduced with permission.[188] Copyright 2015, Royal Society of Chemistry. j) Schematic illustration of the structure of stretchable fiber piezoelectric nanogenerator. Reproduced with permission.[198] Copyright 2015, Wiley-VCH. k) Schematic illustration describing the stretchable fiber triboelectric nanogenerator based on coaxial structure. l) The open-circuit voltages ($V_{OC}$) of the stretchable fiber triboelectric nanogenerator generated under repeated stretching stimulations. (k,l) Reproduced with permission.[192] Copyright 2017, Royal Society of Chemistry. m) Schematic illustration of the structure and operating principle of stretchable fiber integrated energy device consisting of the fiber supercapacitor and fiber solar cell. n) Photocharging and discharging processes of the stretchable fiber integrated energy device before and after stretching under strains of 10%, 20%, 30%, and 40%. (m,n) Reproduced with permission.[201] Copyright 2014, Wiley-VCH.

to the applied strains. In this regard, 1D electrodes with high electrical conductivity and stretchable property is highly desired for achieving stretchable 1D solar cells with high-performance. The wound structure of 1D electrodes, which can retain stable electrical conductivity under tensile strains, are mainly used in the 1D devices.[185–188] Yang et al. developed 1D stretchable dye-sensitized solar cells (DSSCs) by helically winding a Ti wire modified with an aligned TiO$_2$ nanotube array as the anode onto an elastic 1D electrode wrapped with an aligned CNT sheet as the cathode. Subsequently, the DSSCs were coated with photoactive materials (**Figure 10**a,b).[185] The resulting 1D DSSCs exhibited a high energy conversion efficiency of 7.13%. In addition, the efficiency decreased slightly upon a stretching deformation up to 30% and was maintained at 90% after the repeated stretching under 20% strain for 50 cycles (Figure 10c).

Numerous advancements have been made in the field of 1D photovoltaic devices based on liquid electrolytes. However, the replacement of the liquid electrolyte is an important concern owing to limitations such as toxicity, corrosivity of organic solvents, leakage, vaporization, and complicated fabrication.[1,5] Li et al. developed a novel and stable gel electrolyte for stretchable 1D DSSCs by using a highly stable, nonvolatile hydrophobic polymeric ionic liquid gel.[186] Based on the developed gel electrolyte, highly stretchable 1D DSSCs were fabricated by winding the 1D electrodes, followed by coating the developed gel electrolyte (Figure 10d). The designed stretchable 1D DSSCs not only overcame the limitations of the previous 1D DSSCs based on liquid electrolytes, but also showed high flexibility, stretchability, and a power conversion efficiency of 5.47%. In addition, the stretchable 1D polymer solar cells further improved the performance and stability.[5] Zhang et al. demonstrated a flexible and stretchable 1D polymer solar cells based on polymeric photoactive materials and the wound 1D electrodes on an elastic wire substrate (Figure 10e).[187] These 1D polymer solar cells could be further woven into a textile form, exhibiting comparable energy conversion efficiencies that decreases by less than 10% after repeated stretching deformations with the strain of 30% for 50 cycles (Figure 10f).

Although the 1D polymer solar cells have improved the power conversion efficiency of the devices compared to the previous solar cells, the higher performance of the energy devices is still in demand for their practical applications. Due to their remarkable power conversion efficiency, perovskite solar cells have been intensively investigated in the last decade. 1D perovskite solar cells have been also developed based on a coaxial structure or a twisted structure in order to further enhance the energy conversion performance.[173,189–191] However, the efficiencies of the 1D perovskite solar cells are still poor compared to that of planar perovskite solar cells because of the difficulty in achieving high-quality interfaces and uniform morphologies of the photoactive and electrode layers in the 1D solar cells. Deng et al. designed an elastic 1D perovskite solar cells by using a spring-like Ti wire modified with $TiO_2$ and an aligned CNTs-based stretchable wire as the two electrodes (Figure 10g,h).[188] The perovskite material and hole transfer layer were simply coated onto the modified Ti wire electrode through a solution process. The power conversion efficiency of the fabricated 1D perovskite solar cells was not higher (≈1.01%) than that of the existing 1D solar cells, but it could be maintained at 90% after repeated stretching for 250 cycles under 30% strain based on the helically wound structure of the 1D electrode (Figure 10i). However, for their practical applications, stretchable 1D perovskite solar cells still should overcome several challenges such as an unstable property of perovskite salts and high toxicity of Pb.[5,173,190]

Stretchable 1D nanogenerators that convert mechanical energy into electrical energy are also one of the promising 1D energy-harvesting devices.[1,175,192,193] Although the energy-harvesting performance of nanogenerators mainly depends on their active materials and structural designs, the electrical performance of electrodes largely affects the performance of the devices as well.[194–196] In particular, high electrical conductivity of the electrodes in the nanogenerators plays an important role in collecting the generated output current, contributing high output current in an external circuit.[196,197] Therefore, high-performance 1D stretchable electrodes are fundamentally essential for the development of the stretchable 1D nanogenerators. Sim et al. developed a highly flexible and stretchable piezoelectric yarn by using an electrospun polyvinylidene fluoride-*co*-trifluoroethylene (PVDF–TrFE) mat as a piezoelectric material, and silver-coated nylon yarn, and aligned CNT sheet as two electrodes (Figure 10j).[198] The fabricated flexible piezoelectric yarns could be intrinsically stretched up to a tensile strain of only 5% generating over 50 µW cm$^{-3}$; it could be advanced to piezoelectric coils by twist insertion, enabling the 1D nanogenerators to be reversibly stretched up to 50% strain without failure. The triboelectric effect, which refers to contact electrification generated from the frictional contact between two different materials, was also applied to achieve high-performance stretchable 1D nanogenerators.[107,108,199,200] Yu et al. developed an 1D stretchable triboelectric nanogenerator based on a coaxial structure by using two aligned CNT sheets as the inner and outer electrodes on a PDMS wire substrate.[192] PDMS and poly(methyl methacrylate) (PMMA) layers were used as contact materials for triboelectric generation (Figure 10k). In order to improve the output performance, porous microstructures were applied to both PDMS and PMMA layers, and an air gap was designed in the 1D devices to induce rough surfaces and effective contacts. The developed triboelectric yarns effectively generated electric charges from various deformations such as normal pressure, bending, twisting, vibrating, and stretching. In particular, the 1D devices exhibited the maximal output $V_{OC}$ of 1.1 V under repeated stretching and releasing cycles (Figure 10l). To further improve the stretchability of 1D triboelectric nanogenerators, He et al. designed a highly stretchable 1D triboelectric nanogenerator using a Cu wire wound helically on stretchable electrodes on an elastic wire substrate, resulting the high stretchability of up to 70%.[107] In addition, the developed 1D nanogenerators could generate a high maximum $V_{OC}$ of 142.8 V and $Q_{SC}$ of 61 nC per stretching deformation.

Although numerous efforts have been dedicated to realize and maximize the performance of 1D energy storage and harvesting devices, in general, energy harvesting devices require immediate rectification and storage and energy storage devices still should be frequently charged for their practical applications. Hence, integrated energy devices consisting both energy harvesting and storage devices in the same system were designed and developed.[201,202] The electric energy generated from energy-harvesting devices can be simultaneously stored in energy storage devices in integrated systems. Yang et al. developed an 1D stretchable integrated energy device that can generate electric energy from a solar cell part in its sheath and can directly store the generated electric energy into a supercapacitor part in its core.[201] The 1D supercapacitor was fabricated based on aligned CNT sheet electrodes and gel electrolyte on an elastic wire substrate; the 1D solar cell was directly combined by applying another CNT electrode, wound Ti wire electrode, and electrolyte onto the fabricated core storage part (Figure 10m). The developed 1D integrated energy device could effectively maintain its efficiency of energy conversion and storage (1.83%) even after stretching deformations of 10 and 20% (Figure 10n). In addition, the photo-charging and discharging performance of the integrated device remained

**Table 1.** Summary of 1D stretchable electrodes reported in the literature.

| Conductive material | Fabrication technique | Conductivity | Stretchability | Stretching mechanism | Application | Ref. |
|---|---|---|---|---|---|---|
| rGO | Dip coating | 0.02 Ωm | 60% | Structural[a] (Coiled structure) | Electrode | [48] |
| GO | Dip coating | 0.136 S m$^{-1}$ | ≈100% | Structural (Coiled structure) | Bending sensor | [49] |
| MWCNTs &SWCNTs | Dip coating | 13 S cm$^{-1}$ | 100% | Intrinsic[b] | Strain sensor | [55] |
| AgNWs | Dip coating | 5 Ω cm$^{-1}$ | 100% | Intrinsic | Strain sensor | [58] |
| AgNWs | Dip coating | 1 Ω cm$^{-1}$ | 150% | Intrinsic | Strain sensor | [60] |
| SWCNTs | Dip coating | 11.2 kΩ cm$^{-1}$ | 300% | Intrinsic | Strain sensor | [86] |
| AgNPs/Graphene | Dip coating | 423 mS cm$^{-1}$ | 50% | Intrinsic | Strain sensor | [87] |
| CuNWs | Dip coating | 2.5 Ω cm$^{-1}$ | 100% | Structural (Coiled structure) | Textile heater | [63] |
| PEDOT | Dip coating | 600 Ω cm$^{-1}$ | 20% | Intrinsic | Strain sensor | [111] |
| Polypyrrole | Dip coating | – | 100% | Structural (Coiled structure) | Temperature sensor | [124] |
| SWCNTs | Wet spinning | 71 Ω cm$^{-1}$ | 250% | Intrinsic | Strain sensor | [54] |
| AgNWs | Wet spinning | 4962 S cm$^{-1}$ | 200% | Intrinsic | – | [59] |
| Ag nanoflowers | Wet spinning | 41 245 S cm$^{-1}$ | 90% | Intrinsic | – | [62] |
| MWCNTs | Wet spinning | – | 300% | Intrinsic | Strain sensor | [71] |
| Conductive hydrogel | Wet spinning | 2 S cm$^{-1}$ | 500% | Intrinsic | – | [72] |
| AuNWs/AuFilm | Dry spinning | 461 S cm$^{-1}$ | 360% | Structural (Coiled structure) | Electrode | [64] |
| AgNPs | Chemical incorporation | 20 964 S cm$^{-1}$ | 450% | Intrinsic | Strain sensor | [24] |
| FWCNTs | Chemical incorporation | 167.41 S cm$^{-1}$ | 150% | Intrinsic | – | [57] |
| AgNWs/AgNPs | Chemical incorporation | 2450 S cm$^{-1}$ | 220% | Intrinsic | Strain sensor | [61] |
| AgNWs | Thermal drawing, Dip coating | 34 ± 17 kΩ | 100% | Intrinsic | Electrode | [81] |
| EGaIn/CBs | Thermal drawing | 1 Ω m | 500% | Intrinsic | Electrode, Strain sensor | [82] |
| Liquid metal (EGaIn) | Direct injection | 34 000 S cm$^{-1}$ | 700% | Intrinsic | Interconnect | [66] |
| Liquid metal (EGaIn) | Direct injection | – | 100% | Intrinsic | Torsion sensor, Strain sensor | [118] |
| MWCNTs | Wrapping MWCNTs sheet | 26.1 Ω cm$^{-1}$ | 1320% | Structural (Buckled structure) | Strain sensor, Artificial muscle | [99] |
| SWCNTs | Wrapping SWCNTs sheet | 440 S cm$^{-1}$ | 285% | Structural (Spring structure) | Strain sensor | [105] |
| MWCNTs | Wrapping MWCNTs sheet | – | 100% | Intrinsic | Electrode | [154] |
| MWCNTs | Wrapping MWCNTs sheet | 0.19 kΩ cm$^{-1}$ | 160% | Structural (Coiled structure) | Electrode | [167] |
| Au films | Physical deposition | 1.38 Ω cm$^{-1}$ | 80% | Intrinsic | – | [89] |
| Graphene | Chemical vapor deposition | 25 000 S m$^{-1}$ | 7.1% | Intrinsic | Strain sensor | [52] |
| rGO | Twisting rGO films | 60 000 S m$^{-1}$ | 40% | Intrinsic | Textile heater | [50] |
| Cu wires | Helically winding | – | 70% | Structural (Coiled structure) | Electrode | [107] |
| Ionically conductive fluid | Multicore-shell printing | 50 μS cm$^{-1}$ | 700% | Intrinsic | Strain sensor | [113] |

[a]The structural feature is used for stretchability; [b]The electrode is intrinsically stretched.

stable under repeated stretching deformations of 20% strain for 50 cycles. Furthermore, 1D energy harvesting and storage devices can be integrated into one textile by weaving them as the warp and weft yarns. Dong et al. reported a stretchable and washable all-yarn-based integrated energy textile by knitting a fiber triboelectric nanogenerator and 1D supercapacitor into one fabric.[203] Based on the weft-knitting technique, the fabricated energy textile exhibited high flexibility and stretchability

as well as high energy-harvesting and storing performance. In general, while the performance of 1D energy devices is largely affected by the electrical performance of its electrodes, achieving the ideal 1D stretchable electrode that perfectly maintains its electrical conductivity during large stretching deformation remains a great challenge. Therefore, owing to their unique weavable feature, stretchable fiber-integrated energy devices are greatly promising for future wearable or textile energy electronic systems.

## 5. Summary and Outlook

In the past decade, the interdisciplinary research area of 1D electronic devices has rapidly and extensively developed with the advancement of wearable electronics and textile electronics. Furthermore, because the 1D electronic devices should be robust to various mechanical deformations and stimulations in practical applications, 1D stretchable electronic devices which can maintain their high performance under mechanical deformations appear more promising in this research field. In this paper, we systematically summarized the recent technological achievements in 1D stretchable electronic devices in terms of the representative conductive materials and fabrication process for 1D stretchable electrodes, and various electronic devices based on the 1D stretchable electrodes. For realizing high-performance 1D stretchable electrodes and electronic devices, it is crucial that various nanoscaled organic and inorganic materials and their hybrids are introduced for endowing their electrical functions either on the surface or inside a single stretchable fiber matrix. Fabrication techniques for 1D stretchable electrodes are roughly grouped into two categories: applying coating layer or composites of conductive materials to intrinsically stretchable yarn and applying structural features to conductive yarns or conductive layers for realizing high stretchability. In particular, the former approach is described by two groups depending on whether the conductive materials are applied during or after the spinning process of the stretchable 1D matrix. Various 1D stretchable electronic devices including 1D mechanical sensors such as those for measuring strain, pressure, bending, and torsion sensors; wearable heaters; thermal sensors; and energy storage and harvesting devices were also presented. The key features of representative 1D stretchable electrodes including the conductive material, fabrication strategy, electrical conductivity, stretchability, and application are systematically summarized in **Table 1**.

Despite the remarkable advances in 1D stretchable electronics for wearable electronics, several challenges that hinder their practical applications still remain. First, the performance of 1D stretchable electronic devices is still limited to realize a fully integrated electronic system that only consists of 1D electronic components. Due to its fibrous structure, the stretchable conductive yarns for 1D electronic devices can be partially used as interconnects at the same time. Therefore, the connections between the electronic devices and interconnects, generally considered as a severe practical limitation in stretchable electronics, can be removed in 1D electronic systems. For achieving such 1D stretchable electronic systems, various 1D stretchable electronic components such as transistors, antennas, memories, and circuitry should be developed with high performance comparable to that of modern electronic components. However, they are still far away from fulfilling the performance required for practical applications mainly because of the surface roughness of the fibers and the difficulty in achieving high-level micro fabrications on the small and curved surfaces of the fibers. In addition, the electrical performance and stability of 1D stretchable electrodes are also not satisfactory for their practical applications. Thus, a systematic study for the scientific understanding and optimal design of the hierarchy structures and interfacial properties of the fibers is highly desired to achieve 1D electronic systems.

With respect to materials, various materials for 1D stretchable electronic devices should be extended to more broad range of materials, such as biocompatible, biodegradable, and environment-friendly materials, that will not pose any threat to humans or the environment. It is also required in terms of the extension of their applications. On the other hand, to realize the commercial potential of the 1D stretchable electronic devices and systems, practically efficient weaving techniques are fundamentally essential for producing smart textiles. The weaving techniques currently available in the industry are hard to be used for the 1D stretchable electronic devices due to the mechanical properties and stability of the 1D devices.

Up to date, all the research about 1D stretchable electronic devices in this field have mainly focused on the development of each electronic component, such as a capacitor, transistor, diode, various sensors, and energy devices. Therefore, the next step of 1D stretchable electronic devices should be to realize a higher level of electronic devices such as memory devices, logic gates, and complementary metal-oxide-semiconductor devices based on only 1D stretchable electronic components. To successfully combine the existing 1D stretchable electronic devices and overcome the current scientific obstacle in this field, an in-depth understanding of the various mechanisms and fundamentals involved in the complex 1D electronic systems should be achieved. Through such advancement, the 1D stretchable electronic devices and systems are strongly expected to be used as one of the main electronic systems in our daily life.

## Conflict of Interest

The authors declare no conflict of interest.

**ADVANCED
SCIENCE NEWS**

www.advancedsciencenews.com

**ADVANCED
MATERIALS**

www.advmat.de

[1] H. Sun, Y. Zhang, J. Zhang, X. Sun, H. Peng, *Nat. Rev. Mater.* **2017**, *2*, 17023.

[2] S. Bauer, *Nat. Mater.* **2013**, *12*, 871.

[3] W. Zeng, L. Shu, Q. Li, S. Chen, F. Wang, X.-M. Tao, *Adv. Mater.* **2014**, *26*, 5310.

[4] M. Liao, L. Ye, Y. Zhang, T. Chen, H. Peng, *Adv. Electron. Mater.* **2019**, *5*, 1800456.

[5] T. Lv, Y. Yao, N. Li, T. Chen, *Nano Today* **2016**, *11*, 644.

[6] K. Jost, G. Dion, Y. Gogotsi, *J. Mater. Chem. A* **2014**, *2*, 10776.

[7] T. Bashir, M. Ali, N.-K. Persson, S. K. Ramamoorthy, M. Skrifvars, *Text. Res. J.* **2014**, *84*, 323.

[8] E. Nilsson, M. Rigdahl, B. Hagström, *J. Appl. Polym. Sci.* **2015**, *132*, 42255.

[9] M. Åkerfeldt, A. Lund, P. Walkenström, *Text. Res. J.* **2015**, *85*, 1789.

[10] X. Liu, R. Guo, Y. Shi, L. Deng, Y. Li, *Macromol. Mater. Eng.* **2016**, *301*, 1383.

[11] N. Karim, M. Zhang, S. Afroj, V. Koncherry, P. Potluri, K. S. Novoselov, *RSC Adv.* **2018**, *8*, 16815.

[12] M. G. Tadesse, D. A. Mengistie, Y. Chen, L. Wang, C. Loghin, V. Nierstrasz, *J. Mater. Sci.* **2019**, *54*, 9591.

[13] N. Karim, S. Afroj, S. Tan, P. He, A. Fernando, C. Carr, K. S. Novoselov, *ACS Nano* **2017**, *11*, 12266.

[14] M. Papaiordanidou, S. Takamatsu, S. Rezaei-Mazinani, T. Lonjaret, A. Martin, E. Ismailova, *Adv. Healthcare Mater.* **2016**, *5*, 2001.

[15] S. Takamatsu, T. Lonjaret, E. Ismailova, A. Masuda, T. Itoh, G. G. Malliaras, *Adv. Mater.* **2016**, *28*, 4485.

[16] S. Takamatsu, T. Lonjaret, D. Crisp, J.-M. Badier, G. G. Malliaras, E. Ismailova, *Sci. Rep.* **2015**, *5*, 15003.

[17] E. Bihar, T. Roberts, E. Ismailova, M. Saadaoui, M. Isik, A. Sanchez-Sanchez, D. Mecerreyes, T. Hervé, J. B. De Graaf, G. G. Malliaras, *Adv. Mater. Technol.* **2017**, *2*, 1600251.

[18] C. Zhu, X. Guan, X. Wang, Y. Li, E. Chalmers, X. Liu, *Adv. Mater. Interfaces* **2019**, *6*, 1801547.

[19] T. Bashir, M. Skrifvars, N.-K. Persson, *Polym. Adv. Technol.* **2018**, *29*, 310.

[20] D. Janas, S. K. Kreft, K. K. K. Koziol, *Mater. Des.* **2017**, *116*, 16.

[21] E. Nilsson, H. Oxfall, W. Wandelt, R. Rychwalski, B. Hagström, *J. Appl. Polym. Sci.* **2013**, *130*, 2579.

[22] M. M. B. Hasan, A. Matthes, P. Schneider, C. Cherif, *Mater. Technol.* **2011**, *26*, 128.

[23] S. Hooshmand, A. Soroudi, M. Skrifvars, *Synth. Met.* **2011**, *161*, 1731.

[24] J. Lee, S. Shin, S. Lee, J. Song, S. Kang, H. Han, S. Kim, S. Kim, J. Seo, D. Kim, T. Lee, *ACS Nano* **2018**, *12*, 4259.

[25] S. Coyle, King-Tong Lau, N. Moyna, D. O'Gorman, D. Diamond, F. Di Francesco, D. Costanzo, P. Salvo, M. G. Trivella, D. E. De Rossi, N. Taccini, R. Paradiso, J.-A. Porchet, A. Ridolfi, J. Luprano, C. Chuzel, T. Lanier, F. Revol-Cavalier, S. Schoumacker, V. Mourier, I. Chartier, R. Convert, H. De-Moncuit, C. Bini, *IEEE Trans. Inf. Technol. Biomed.* **2010**, *14*, 364.

[26] M. Stoppa, A. Chiolerio, M. Stoppa, A. Chiolerio, *Sensors* **2014**, *14*, 11957.

[27] K. Laxminarayana, N. Jalili, *Text. Res. J.* **2005**, *75*, 670.

[28] M. Kaltenbrunner, T. Sekitani, J. Reeder, T. Yokota, K. Kuribara, T. Tokuhara, M. Drack, R. Schwödiauer, I. Graz, S. Bauer-Gogonea, S. Bauer, T. Someya, *Nature* **2013**, *499*, 458.

[29] M. Parrilla, R. Cánovas, I. Jeerapan, F. J. Andrade, J. Wang, *Adv. Healthcare Mater.* **2016**, *5*, 996.

[30] Z. Li, Z. L. Wang, *Adv. Mater.* **2011**, *23*, 84.

[31] K. Cherenack, C. Zysset, T. Kinkeldei, N. Münzenrieder, G. Tröster, *Adv. Mater.* **2010**, *22*, 5178.

[32] F. Clemens, M. Wegmann, T. Graule, A. Mathewson, T. Healy, J. Donnelly, A. Ullsperger, W. Hartmann, C. Papadas, *Adv. Eng. Mater.* **2003**, *5*, 682.

[33] Y. Fu, X. Cai, H. Wu, Z. Lv, S. Hou, M. Peng, X. Yu, D. Zou, *Adv. Mater.* **2012**, *24*, 5713.

[34] N. Liu, W. Ma, J. Tao, X. Zhang, J. Su, L. Li, C. Yang, Y. Gao, D. Golberg, Y. Bando, *Adv. Mater.* **2013**, *25*, 4925.

[35] M. Park, J. Im, M. Shin, Y. Min, J. Park, H. Cho, S. Park, M.-B. Shim, S. Jeon, D.-Y. Chung, J. Bae, J. Park, U. Jeong, K. Kim, *Nat. Nanotechnol.* **2012**, *7*, 803.

[36] D.-H. Kim, Y.-S. Kim, J. Wu, Z. Liu, J. Song, H.-S. Kim, Y. Y. Huang, K.-C. Hwang, J. A. Rogers, *Adv. Mater.* **2009**, *21*, 3703.

[37] X. Wang, Z. Liu, T. Zhang, *Small* **2017**, *13*, 1602790.

[38] T. Q. Trung, N.-E. Lee, *Adv. Mater.* **2017**, *29*, 1603167.

[39] D.-H. Kim, J. Xiao, J. Song, Y. Huang, J. A. Rogers, *Adv. Mater.* **2010**, *22*, 2108.

[40] T. Sekitani, T. Someya, *Adv. Mater.* **2010**, *22*, 2228.

[41] J. A. Rogers, T. Someya, Y. Huang, *Science* **2010**, *327*, 1603.

[42] S. Yao, Y. Zhu, *Adv. Mater.* **2015**, *27*, 1480.

[43] M. Zhang, C. Wang, H. Wang, M. Jian, X. Hao, Y. Zhang, *Adv. Funct. Mater.* **2017**, *27*, 1604795.

[44] C. Wang, X. Li, E. Gao, M. Jian, K. Xia, Q. Wang, Z. Xu, T. Ren, Y. Zhang, *Adv. Mater.* **2016**, *28*, 6640.

[45] A. Hirsch, *Nat. Mater.* **2010**, *9*, 868.

[46] S. Stankovich, D. A. Dikin, G. H. B. Dommett, K. M. Kohlhaas, E. J. Zimney, E. A. Stach, R. D. Piner, S. T. Nguyen, R. S. Ruoff, *Nature* **2006**, *442*, 282.

[47] R. S. Edwards, K. S. Coleman, *Nanoscale* **2013**, *5*, 38.

[48] Q. Li, K. Li, H. Fan, C. Hou, Y. Li, Q. Zhang, H. Wang, *J. Mater. Chem. C* **2017**, *5*, 11448.

[49] Y. Cheng, R. Wang, J. Sun, L. Gao, *Adv. Mater.* **2015**, *27*, 7365.

[50] R. Wang, Z. Xu, J. Zhuang, Z. Liu, L. Peng, Z. Li, Y. Liu, W. Gao, C. Gao, *Adv. Electron. Mater.* **2017**, *3*, 1600425.

[51] S. Wang, N. Liu, J. Su, L. Li, F. Long, Z. Zou, X. Jiang, Y. Gao, *ACS Nano* **2017**, *11*, 2066.

[52] X. Wang, Y. Qiu, W. Cao, P. Hu, *Chem. Mater.* **2015**, *27*, 6969.

[53] T. W. Ebbesen, H. J. Lezec, H. Hiura, J. W. Bennett, H. F. Ghaemi, T. Thio, *Nature* **1996**, *382*, 54.

[54] J. Zhou, X. Xu, Y. Xin, G. Lubineau, *Adv. Funct. Mater.* **2018**, *28*, 1705591.

[55] Y. Li, B. Zhou, G. Zheng, X. Liu, T. Li, C. Yan, C. Cheng, K. Dai, C. Liu, C. Shen, Z. Guo, *J. Mater. Chem. C* **2018**, *6*, 2258.

[56] L. Jiao, L. Zhang, X. Wang, G. Diankov, H. Dai, *Nature* **2009**, *458*, 877.

[57] S. Jiang, H. Zhang, S. Song, Y. Ma, J. Li, G. H. Lee, Q. Han, J. Liu, *ACS Nano* **2015**, *9*, 10252.

[58] S. Chen, Z. Lou, D. Chen, K. Jiang, G. Shen, *Adv. Mater. Technol.* **2016**, *1*, 1600136.

[59] Y. Lu, J. Jiang, S. Yoon, K.-S. Kim, J.-H. Kim, S. Park, S.-H. Kim, L. Piao, *ACS Appl. Mater. Interfaces* **2018**, *10*, 2093.

[60] Z. Cao, R. Wang, T. He, F. Xu, J. Sun, *ACS Appl. Mater. Interfaces* **2018**, *10*, 14087.

[61] S. Lee, S. Shin, S. Lee, J. Seo, J. Lee, S. Son, H. J. Cho, H. Algadi, S. Al-Sayari, D. E. Kim, T. Lee, *Adv. Funct. Mater.* **2015**, *25*, 3114.

[62] R. Ma, B. Kang, S. Cho, M. Choi, S. Baik, *ACS Nano* **2015**, *9*, 10876.

[63] Y. Cheng, H. Zhang, R. Wang, X. Wang, H. Zhai, T. Wang, Q. Jin, J. Sun, *ACS Appl. Mater. Interfaces* **2016**, *8*, 32925.

[64] Y. Zhao, D. Dong, S. Gong, L. Brassart, Y. Wang, T. An, W. Cheng, *Adv. Electron. Mater.* **2019**, *5*, 1800462.

[65] N. W. Ashcroft, J. Lekner, *Phys. Rev.* **1966**, *145*, 83.

[66] S. Zhu, J.-H. So, R. Mays, S. Desai, W. R. Barnes, B. Pourdeyhimi, M. D. Dickey, *Adv. Funct. Mater.* **2013**, *23*, 2308.

[67] J. Tersoff, *Appl. Phys. Lett.* **1999**, *74*, 2122.

[68] A. J. Granero, P. Wagner, K. Wagner, J. M. Razal, G. G. Wallace, M. in het Panhuis, *Adv. Funct. Mater.* **2011**, *21*, 955.

[69] R. Jalili, S. H. Aboutalebi, D. Esrafilzadeh, R. L. Shepherd, J. Chen, S. Aminorroaya-Yamini, K. Konstantinov, A. I. Minett, J. M. Razal, G. G. Wallace, *Adv. Funct. Mater.* **2013**, *23*, 5345.

[70] I. Marriam, X. Wang, M. Tebyetekerwa, G. Chen, F. Zabihi, J. Pionteck, S. Peng, S. Ramakrishna, S. Yang, M. Zhu, *J. Mater. Chem. A* **2018**, *6*, 13633.

[71] Z. Tang, S. Jia, F. Wang, C. Bian, Y. Chen, Y. Wang, B. Li, *ACS Appl. Mater. Interfaces* **2018**, *10*, 6624.

[72] X. Zhao, F. Chen, Y. Li, H. Lu, N. Zhang, M. Ma, *Nat. Commun.* **2018**, *9*, 3579.

[73] J. Eom, Y. R. Lee, J. H. Lee, S. K. Park, Y. Jeong, J. S. Park, Y.-H. Kim, *Compos. Sci. Technol.* **2019**, *169*, 1.

[74] M. Zhang, C. Wang, Q. Wang, M. Jian, Y. Zhang, *ACS Appl. Mater. Interfaces* **2016**, *8*, 20894.

[75] J. Guo, X. Liu, N. Jiang, A. K. Yetisen, H. Yuk, C. Yang, A. Khademhosseini, X. Zhao, S.-H. Yun, *Adv. Mater.* **2016**, *28*, 10244.

[76] Y. Qu, N. Bartolomei, M. Lagier, T. Nguyen-Dang, A. G. Page, W. Yan, T. Das Gupta, F. Sorin, in *Adv. Photonics 2018 (BGPP, IPR, NP, NOMA, Sensors, Networks, SPPCom, SOF)*, Optical Society Of America, Zurich **2018**, p. SoW1H.3.

[77] T. Khudiyev, C. Hou, A. M. Stolyarov, Y. Fink, *Adv. Mater.* **2017**, *29*, 1605868.

[78] M. Bayindir, F. Sorin, A. F. Abouraddy, J. Viens, S. D. Hart, J. D. Joannopoulos, Y. Fink, *Nature* **2004**, *431*, 826.

[79] A. F. Abouraddy, M. Bayindir, G. Benoit, S. D. Hart, K. Kuriki, N. Orf, O. Shapira, F. Sorin, B. Temelkuran, Y. Fink, *Nat. Mater.* **2007**, *6*, 336.

[80] F. Sordo, E.-R. Janecek, Y. Qu, V. Michaud, F. Stellacci, J. Engmann, T. J. Wooster, F. Sorin, *Adv. Mater.31*, **2019**, 1807282.

[81] C. Lu, S. Park, T. J. Richner, A. Derry, I. Brown, C. Hou, S. Rao, J. Kang, C. T. Mortiz, Y. Fink, P. Anikeeva, *Sci. Adv.* **2017**, *3*, e1600955.

[82] Y. Qu, T. Nguyen-Dang, A. G. Page, W. Yan, T. Das Gupta, G. M. Rotaru, R. M. Rossi, V. D. Favrod, N. Bartolomei, F. Sorin, *Adv. Mater.* **2018**, *30*, 1707251.

[83] Q. Chen, D. Xiang, L. Wang, Y. Tang, E. Harkin-Jones, C. Zhao, Y. Li, *Composites, Part A* **2018**, *112*, 186.

[84] A. Ali, V. Baheti, J. Militky, Z. Khan, S. Q. Z. Gilani, *Fibers Polym.* **2018**, *19*, 607.

[85] D. Hu, X. Xu, J. Miao, O. Gidron, H. Meng, *Materials* **2018**, *11*, 184.

[86] Z. Wang, Y. Huang, J. Sun, Y. Huang, H. Hu, R. Jiang, W. Gai, G. Li, C. Zhi, *ACS Appl. Mater. Interfaces* **2016**, *8*, 24837.

[87] X. Li, H. Hu, T. Hua, B. Xu, S. Jiang, *Nano Res.* **2018**, *11*, 5799.

[88] Y. Tao, Y. Liu, H. Zhang, C. A. Stevens, E. Bilotti, T. Peijs, J. J. C. Busfield, *Compos. Sci. Technol.* **2018**, *167*, 24.

[89] B. Zhang, J. Lei, D. Qi, Z. Liu, Y. Wang, G. Xiao, J. Wu, W. Zhang, F. Huo, X. Chen, *Adv. Funct. Mater.* **2018**, *28*, 1801683.

[90] J. Lee, H. Kwon, J. Seo, S. Shin, J. H. Koo, C. Pang, S. Son, J. H. Kim, Y. H. Jang, D. E. Kim, T. Lee, *Adv. Mater.* **2015**, *27*, 2433.

[91] V. K. S. Shante, S. Kirkpatrick, *Adv. Phys.* **1971**, *20*, 325.

[92] Y. Kim, J. Zhu, B. Yeom, M. Di Prima, X. Su, J.-G. Kim, S. J. Yoo, C. Uher, N. A. Kotov, *Nature* **2013**, *500*, 59.

[93] K.-Y. Chun, Y. Oh, J. Rho, J.-H. Ahn, Y.-J. Kim, H. R. Choi, S. Baik, *Nat. Nanotechnol.* **2010**, *5*, 853.

[94] R. Cruz-Silva, A. Morelos-Gomez, H. Kim, H. Jang, F. Tristan, S. Vega-Diaz, L. P. Rajukumar, A. L. Elías, N. Perea-Lopez, J. Suhr, M. Endo, M. Terrones, *ACS Nano* **2014**, *8*, 5959.

[95] N. Nan, J. He, X. You, X. Sun, Y. Zhou, K. Qi, W. Shao, F. Liu, Y. Chu, B. Ding, *Adv. Mater. Technol.* **2019**, *4*, 1800338.

[96] Y. Zhang, W. Bai, J. Ren, W. Weng, H. Lin, Z. Zhang, H. Peng, *J. Mater. Chem. A* **2014**, *2*, 11054.

[97] C. Choi, J. H. Kim, H. J. Sim, J. Di, R. H. Baughman, S. J. Kim, *Adv. Energy Mater.* **2017**, *7*, 1602021.

[98] C. Choi, J. M. Lee, S. H. Kim, S. J. Kim, J. Di, R. H. Baughman, *Nano Lett.* **2016**, *16*, 7677.

[99] Z. F. Liu, S. Fang, F. A. Moura, J. N. Ding, N. Jiang, J. Di, M. Zhang, X. Lepró, D. S. Galvão, C. S. Haines, N. Y. Yuan, S. G. Yin, D. W. Lee, R. Wang, H. Y. Wang, W. Lv, C. Dong, R. C. Zhang, M. J. Chen, Q. Yin, Y. T. Chong, R. Zhang, X. Wang, M. D. Lima, R. Ovalle-Robles, D. Qian, H. Lu, R. H. Baughman, *Science* **2015**, *349*, 400.

[100] Y. Zhang, W. Bai, X. Cheng, J. Ren, W. Weng, P. Chen, X. Fang, Z. Zhang, H. Peng, *Angew. Chem., Int. Ed.* **2014**, *53*, 14564.

[101] H. Jin, L. Zhou, C. L. Mak, H. Huang, W. M. Tang, H. L. W. Chan, *Nano Energy* **2015**, *11*, 662.

[102] Q. Zhang, J. Sun, Z. Pan, J. Zhang, J. Zhao, X. Wang, C. Zhang, Y. Yao, W. Lu, Q. Li, Y. Zhang, Z. Zhang, *Nano Energy* **2017**, *39*, 219.

[103] A. M. Zamarayeva, A. E. Ostfeld, M. Wang, J. K. Duey, I. Deckman, B. P. Lechêne, G. Davies, D. A. Steingart, A. C. Arias, *Sci. Adv.* **2017**, *3*, e1602051.

[104] P. Liu, Y. Li, Y. Xu, L. Bao, L. Wang, J. Pan, Z. Zhang, X. Sun, H. Peng, *Small* **2018**, *14*, 1702926.

[105] Y. Shang, X. He, Y. Li, L. Zhang, Z. Li, C. Ji, E. Shi, P. Li, K. Zhu, Q. Peng, C. Wang, X. Zhang, R. Wang, J. Wei, K. Wang, H. Zhu, D. Wu, A. Cao, *Adv. Mater.* **2012**, *24*, 2896.

[106] Y. Xu, Y. Zhang, Z. Guo, J. Ren, Y. Wang, H. Peng, *Angew. Chem.* **2015**, *127*, 15610.

[107] X. He, Y. Zi, H. Guo, H. Zheng, Y. Xi, C. Wu, J. Wang, W. Zhang, C. Lu, Z. L. Wang, *Adv. Funct. Mater.* **2017**, *27*, 1604378.

[108] J. Zhong, Q. Zhong, Q. Hu, N. Wu, W. Li, B. Wang, B. Hu, J. Zhou, *Adv. Funct. Mater.* **2015**, *25*, 1798.

[109] Y. Cheng, R. Wang, H. Zhai, J. Sun, *Nanoscale* **2017**, *9*, 3834.

[110] Y. Zhou, J. He, H. Wang, K. Qi, N. Nan, X. You, W. Shao, L. Wang, B. Ding, S. Cui, *Sci. Rep.* **2017**, *7*, 12949.

[111] J. Eom, R. Jaisutti, H. Lee, W. Lee, J.-S. Heo, J.-Y. Lee, S. K. Park, Y.-H. Kim, *ACS Appl. Mater. Interfaces* **2017**, *9*, 10190.

[112] C. Forró, L. Demkó, S. Weydert, J. Vörös, K. Tybrandt, *ACS Nano* **2018**, *12*, 11080.

[113] A. Frutiger, J. T. Muth, D. M. Vogt, Y. Mengüç, A. Campo, A. D. Valentine, C. J. Walsh, J. A. Lewis, *Adv. Mater.* **2015**, *27*, 2440.

[114] H. Wang, Z. Liu, J. Ding, X. Lepró, S. Fang, N. Jiang, N. Yuan, R. Wang, Q. Yin, W. Lv, Z. Liu, M. Zhang, R. Ovalle-Robles, K. Inoue, S. Yin, R. H. Baughman, *Adv. Mater.* **2016**, *28*, 4998.

[115] X. Wu, Y. Han, X. Zhang, C. Lu, *ACS Appl. Mater. Interfaces* **2016**, *8*, 9936.

[116] Y.-Q. Li, P. Huang, W.-B. Zhu, S.-Y. Fu, N. Hu, K. Liao, *Sci. Rep.* **2017**, *7*, 45013.

[117] Y. Wei, S. Chen, X. Yuan, P. Wang, L. Liu, *Adv. Funct. Mater.* **2016**, *26*, 5078.

[118] C. B. Cooper, K. Arutselvan, Y. Liu, D. Armstrong, Y. Lin, M. R. Khan, J. Genzer, M. D. Dickey, *Adv. Funct. Mater.* **2017**, *27*, 1605630.

[119] R. Wang, N. Jiang, J. Su, Q. Yin, Y. Zhang, Z. Liu, H. Lin, F. A. Moura, N. Yuan, S. Roth, R. S. Rome, R. Ovalle-Robles, K. Inoue, S. Yin, S. Fang, W. Wang, J. Ding, L. Shi, R. H. Baughman, Z. Liu, *Adv. Funct. Mater.* **2017**, *27*, 1702134.

**ADVANCED
SCIENCE NEWS**

www.advancedsciencenews.com

**ADVANCED
MATERIALS**

www.advmat.de

[120] L. Yu, J. C. Yeo, R. H. Soon, T. Yeo, H. H. Lee, C. T. Lim, *ACS Appl. Mater. Interfaces* **2018**, *10*, 12773.

[121] S. Chen, H. Liu, S. Liu, P. Wang, S. Zeng, L. Sun, L. Liu, *ACS Appl. Mater. Interfaces* **2018**, *10*, 4305.

[122] J. Di, X. Zhang, Z. Yong, Y. Zhang, D. Li, R. Li, Q. Li, *Adv. Mater.* **2016**, *28*, 10529.

[123] T. Dinh, H.-P. Phan, T.-K. Nguyen, A. Qamar, A. R. M. Foisal, T. Nguyen Viet, C.-D. Tran, Y. Zhu, N.-T. Nguyen, D. V. Dao, *J. Mater. Chem. C* **2016**, *4*, 10061.

[124] Y. He, Q. Gui, S. Liao, H. Jia, Y. Wang, *Adv. Mater. Technol.* **2016**, *1*, 1600170.

[125] C. Hua, Y. Shang, X. Li, X. Hu, Y. Wang, X. Wang, Y. Zhang, X. Li, H. Duan, A. Cao, *Nanoscale* **2016**, *8*, 10659.

[126] X. Liao, Q. Liao, Z. Zhang, X. Yan, Q. Liang, Q. Wang, M. Li, Y. Zhang, *Adv. Funct. Mater.* **2016**, *26*, 3074.

[127] B. Weintraub, Y. Wei, Z. Wang, *Angew. Chem.* **2009**, *121*, 9143.

[128] M. R. Lee, R. D. Eckert, K. Forberich, G. Dennler, C. J. Brabec, R. A. Gaudiana, *Science* **2009**, *324*, 232.

[129] J. Bae, M. K. Song, Y. J. Park, J. M. Kim, M. Liu, Z. L. Wang, *Angew. Chem., Int. Ed.* **2011**, *50*, 1683.

[130] L. Liu, Y. Yu, C. Yan, K. Li, Z. Zheng, *Nat. Commun.* **2015**, *6*, 7260.

[131] Q. Zhou, C. Jia, X. Ye, Z. Tang, Z. Wan, *J. Power Sources* **2016**, *327*, 365.

[132] Z. Yang, J. Ren, Z. Zhang, X. Chen, G. Guan, L. Qiu, Y. Zhang, H. Peng, *Chem. Rev.* **2015**, *115*, 5159.

[133] T. Chen, S. Wang, Z. Yang, Q. Feng, X. Sun, L. Li, Z.-S. Wang, H. Peng, *Angew. Chem.* **2011**, *123*, 1855.

[134] Z. Xu, C. Gao, *Nat. Commun.* **2011**, *2*, 571.

[135] B. Wang, X. Fang, H. Sun, S. He, J. Ren, Y. Zhang, H. Peng, *Adv. Mater.* **2015**, *27*, 7854.

[136] Y. Ai, Z. Lou, L. Li, S. Chen, H. S. Park, Z. M. Wang, G. Shen, *Adv. Mater. Technol.* **2016**, *1*, 1600142.

[137] Z. Cai, L. Li, J. Ren, L. Qiu, H. Lin, H. Peng, *J. Mater. Chem. A* **2013**, *1*, 258.

[138] Z. Lu, J. Foroughi, C. Wang, H. Long, G. G. Wallace, *Adv. Energy Mater.* **2018**, *8*, 1702047.

[139] H. Sun, X. Fu, S. Xie, Y. Jiang, H. Peng, *Adv. Mater.* **2016**, *28*, 2070.

[140] K. Wang, Q. Meng, Y. Zhang, Z. Wei, M. Miao, *Adv. Mater.* **2013**, *25*, 1494.

[141] H. Wu, Z. Lou, H. Yang, G. Shen, *Nanoscale* **2015**, *7*, 1921.

[142] D. Yu, K. Goh, Q. Zhang, L. Wei, H. Wang, W. Jiang, Y. Chen, *Adv. Mater.* **2014**, *26*, 6790.

[143] X. Ouyang, G. Shen, D. Chen, Q. Wang, J. Xu, X. Wang, X. Hou, R. Wang, *Nano Energy* **2014**, *8*, 44.

[144] C. Choi, J. A. Lee, A. Y. Choi, Y. T. Kim, X. Leprō, M. D. Lima, R. H. Baughman, S. J. Kim, *Adv. Mater.* **2014**, *26*, 2059.

[145] B. Liu, B. Liu, X. Wang, D. Chen, Z. Fan, G. Shen, *Nano Energy* **2014**, *10*, 99.

[146] J. Ren, W. Bai, G. Guan, Y. Zhang, H. Peng, *Adv. Mater.* **2013**, *25*, 5965.

[147] J. Ren, L. Li, C. Chen, X. Chen, Z. Cai, L. Qiu, Y. Wang, X. Zhu, H. Peng, *Adv. Mater.* **2013**, *25*, 1155.

[148] J. Ren, Y. Zhang, W. Bai, X. Chen, Z. Zhang, X. Fang, W. Weng, Y. Wang, H. Peng, *Angew. Chem.* **2014**, *126*, 7998.

[149] H. Lin, W. Weng, J. Ren, L. Qiu, Z. Zhang, P. Chen, X. Chen, J. Deng, Y. Wang, H. Peng, *Adv. Mater.* **2014**, *26*, 1217.

[150] W. Weng, Q. Sun, Y. Zhang, H. Lin, J. Ren, X. Lu, M. Wang, H. Peng, *Nano Lett.* **2014**, *14*, 3432.

[151] Y. Zhang, Y. Wang, L. Wang, C.-M. Lo, Y. Zhao, Y. Jiao, G. Zheng, H. Peng, *J. Mater. Chem. A* **2016**, *4*, 9002.

[152] X. Fang, W. Weng, J. Ren, H. Peng, *Adv. Mater.* **2016**, *28*, 491.

[153] Y. Zhang, L. Wang, Z. Guo, Y. Xu, Y. Wang, H. Peng, *Angew. Chem., Int. Ed.* **2016**, *55*, 4487.

[154] Z. Yang, J. Deng, X. Chen, J. Ren, H. Peng, *Angew. Chem., Int. Ed.* **2013**, *52*, 13453.

[155] Z. Zhang, J. Deng, X. Li, Z. Yang, S. He, X. Chen, G. Guan, J. Ren, H. Peng, *Adv. Mater.* **2015**, *27*, 356.

[156] P. Xu, T. Gu, Z. Cao, B. Wei, J. Yu, F. Li, J.-H. Byun, W. Lu, Q. Li, T.-W. Chou, *Adv. Energy Mater.* **2014**, *4*, 1300759.

[157] T. Chen, R. Hao, H. Peng, L. Dai, *Angew. Chem., Int. Ed.* **2015**, *54*, 618.

[158] J. Sun, Y. Huang, C. Fu, Z. Wang, Y. Huang, M. Zhu, C. Zhi, H. Hu, *Nano Energy* **2016**, *27*, 230.

[159] X. Zhang, Q. Li, Y. Tu, Y. Li, J. Y. Coulter, L. Zheng, Y. Zhao, Q. Jia, D. E. Peterson, Y. Zhu, *Small* **2007**, *3*, 244.

[160] J. Cheng, Q. Guan, H. Huang, Z. Wang, S. He, Y. Li, W. Ni, B. Wang, H. Peng, J. Zhou, *Nano Energy* **2018**, *45*, 37.

[161] Y. Zhao, D. Dong, Y. Wang, S. Gong, T. An, L. W. Yap, W. Cheng, *ACS Appl. Mater. Interfaces* **2018**, *10*, 42612.

[162] H. Wang, C. Wang, M. Jian, Q. Wang, K. Xia, Z. Yin, M. Zhang, X. Liang, Y. Zhang, *Nano Res.* **2018**, *11*, 2347.

[163] P. Xu, B. Wei, Z. Cao, J. Zheng, K. Gong, F. Li, J. Yu, Q. Li, W. Lu, J.-H. Byun, B.-S. Kim, Y. Yan, T.-W. Chou, *ACS Nano* **2015**, *9*, 6088.

[164] M. Li, M. Zu, J. Yu, H. Cheng, Q. Li, *Small* **2017**, *13*, 1602994.

[165] J. Yu, W. Lu, J. P. Smith, K. S. Booksh, L. Meng, Y. Huang, Q. Li, J.-H. Byun, Y. Oh, Y. Yan, T.-W. Chou, *Adv. Energy Mater.* **2017**, *7*, 1600976.

[166] P. Li, Z. Jin, L. Peng, F. Zhao, D. Xiao, Y. Jin, G. Yu, *Adv. Mater.* **2018**, *30*, 1800124.

[167] C. Choi, S. H. Kim, H. J. Sim, J. A. Lee, A. Y. Choi, Y. T. Kim, X. Lepró, G. M. Spinks, R. H. Baughman, S. J. Kim, *Sci. Rep.* **2015**, *5*, 9387.

[168] Y. Meng, Y. Zhao, C. Hu, H. Cheng, Y. Hu, Z. Zhang, G. Shi, L. Qu, *Adv. Mater.* **2013**, *25*, 2326.

[169] Y. Shang, C. Wang, X. He, J. Li, Q. Peng, E. Shi, R. Wang, S. Du, A. Cao, Y. Li, *Nano Energy* **2015**, *12*, 401.

[170] Y. Shang, C. Hua, W. Xu, X. Hu, Y. Wang, Y. Zhou, Y. Zhang, X. Li, A. Cao, *Nano Lett.* **2016**, *16*, 1768.

[171] J. Deng, Y. Xu, S. He, P. Chen, L. Bao, Y. Hu, B. Wang, X. Sun, H. Peng, *Nat. Protoc.* **2017**, *12*, 1349.

[172] J. Chen, Y. Huang, N. Zhang, H. Zou, R. Liu, C. Tao, X. Fan, Z. L. Wang, *Nat. Energy* **2016**, *1*, 16138.

[173] L. Qiu, S. He, J. Yang, J. Deng, H. Peng, *Small* **2016**, *12*, 2419.

[174] H. Sun, H. Li, X. You, Z. Yang, J. Deng, L. Qiu, H. Peng, *J. Mater. Chem. A* **2014**, *2*, 345.

[175] X. Li, Z.-H. Lin, G. Cheng, X. Wen, Y. Liu, S. Niu, Z. L. Wang, *ACS Nano* **2014**, *8*, 10674.

[176] T. Chen, L. Qiu, Z. Cai, F. Gong, Z. Yang, Z. Wang, H. Peng, *Nano Lett.* **2012**, *12*, 2568.

[177] T. Chen, L. Qiu, H. Li, H. Peng, *J. Mater. Chem.* **2012**, *22*, 23655.

[178] X. Fan, Z. Z. Chu, F. Z. Wang, C. Zhang, L. Chen, Y. W. Tang, D. C. Zou, *Adv. Mater.* **2008**, *20*, 592.

[179] J. Liu, M. A. G. Namboothiry, D. L. Carroll, *Appl. Phys. Lett.* **2007**, *90*, 133515.

[180] J. Zhong, Y. Zhang, Q. Zhong, Q. Hu, B. Hu, Z. L. Wang, J. Zhou, *ACS Nano* **2014**, *8*, 6273.

[181] D. J. Lipomi, B. C.-K. Tee, M. Vosgueritchian, Z. Bao, *Adv. Mater.* **2011**, *23*, 1771.

[182] D. J. Lipomi, Z. Bao, *Energy Environ. Sci.* **2011**, *4*, 3314.

[183] J. Ryu, J. Kim, J. Oh, S. Lim, J. Y. Sim, J. S. Jeon, K. No, S. Park, S. Hong, *Nano Energy* **2019**, *55*, 348.

[184] Q. Zhang, L. Li, H. Li, L. Tang, B. He, C. Li, Z. Pan, Z. Zhou, Q. Li, J. Sun, L. Wei, X. Fan, T. Zhang, Y. Yao, *Nano Energy* **2019**, *60*, 267.

[185] Z. Yang, J. Deng, X. Sun, H. Li, H. Peng, *Adv. Mater.* **2014**, *26*, 2643.

[186] H. Li, J. Guo, H. Sun, X. Fang, D. Wang, H. Peng, *ChemNanoMat* **2015**, *1*, 399.

[187] Z. Zhang, Z. Yang, J. Deng, Y. Zhang, G. Guan, H. Peng, *Small* **2015**, *11*, 675.

**ADVANCED
SCIENCE NEWS**

www.advancedsciencenews.com

**ADVANCED
MATERIALS**

www.advmat.de

[188] J. Deng, L. Qiu, X. Lu, Z. Yang, G. Guan, Z. Zhang, H. Peng, *J. Mater. Chem. A* **2015**, *3*, 21070.

[189] M. Lee, Y. Ko, Y. Jun, *J. Mater. Chem. A* **2015**, *3*, 19310.

[190] R. Li, X. Xiang, X. Tong, J. Zou, Q. Li, *Adv. Mater.* **2015**, *27*, 3831.

[191] L. Qiu, J. Deng, X. Lu, Z. Yang, H. Peng, *Angew. Chem., Int. Ed.* **2014**, *53*, 10425.

[192] X. Yu, J. Pan, J. Zhang, H. Sun, S. He, L. Qiu, H. Lou, X. Sun, H. Peng, *J. Mater. Chem. A* **2017**, *5*, 6032.

[193] W. Zeng, X.-M. Tao, S. Chen, S. Shang, H. L. W. Chan, S. H. Choy, *Energy Environ. Sci.* **2013**, *6*, 2631.

[194] Z. L. Wang, J. Chen, L. Lin, *Energy Environ. Sci.* **2015**, *8*, 2250.

[195] F. R. Fan, W. Tang, Z. L. Wang, *Adv. Mater.* **2016**, *28*, 4283.

[196] B. Kumar, S.-W. Kim, *J. Mater. Chem.* **2011**, *21*, 18946.

[197] H.-J. Shin, W. M. Choi, D. Choi, G. H. Han, S.-M. Yoon, H.-K. Park, S.-W. Kim, Y. W. Jin, S. Y. Lee, J. M. Kim, J.-Y. Choi, Y. H. Lee, *J. Am. Chem. Soc.* **2010**, *132*, 15603.

[198] H. J. Sim, C. Choi, C. J. Lee, Y. T. Kim, G. M. Spinks, M. D. Lima, R. H. Baughman, S. J. Kim, *Adv. Eng. Mater.* **2015**, *17*, 1270.

[199] Y. Cheng, X. Lu, K. Hoe Chan, R. Wang, Z. Cao, J. Sun, G. Wei Ho, *Nano Energy* **2017**, *41*, 511.

[200] Y.-C. Lai, J. Deng, S. L. Zhang, S. Niu, H. Guo, Z. L. Wang, *Adv. Funct. Mater.* **2017**, *27*, 1604462.

[201] Z. Yang, J. Deng, H. Sun, J. Ren, S. Pan, H. Peng, *Adv. Mater.* **2014**, *26*, 7038.

[202] Z. Zhang, X. Chen, P. Chen, G. Guan, L. Qiu, H. Lin, Z. Yang, W. Bai, Y. Luo, H. Peng, *Adv. Mater.* **2014**, *26*, 466.

[203] K. Dong, Y. C. Wang, J. Deng, Y. Dai, S. L. Zhang, H. Zou, B. Gu, B. Sun, Z. L. Wang, *ACS Nano* **2017**, *11*, 9490.